ELSEVIER

Hyperspectral Vegetation Indices and Their Relationships with Agricultural Crop Characteristics

*Prasad S. Thenkabail**, *Ronald B. Smith** *and Eddy De Pauw*†

The objective of this paper is to determine spectral bands that are best suited for characterizing agricultural crop biophysical variables. The data for this study comes from ground-level hyperspectral reflectance measurements of cotton, potato, soybeans, corn, and sunflower. Reflectance was measured in 490 discrete narrow bands between 350 and 1,050 nm. Observed crop characteristics included wet biomass, leaf area index, plant height, and (for cotton only) yield. Three types of hyperspectral predictors were tested: optimum multiple narrow band reflectance (OMNBR), narrow band normalized difference vegetation index (NDVI) involving all possible two-band combinations of 490 channels, and the soil-adjusted vegetation indices. A critical problem with OMNBR models was that of "over fitting" (i.e., using more spectral channels than experimental samples to obtain a highly maximum R^2 *value). This problem was addressed by comparing the* R^2 *values of crop variables with the* R^2 *values computed for random data of a large sample size. The combinations of two to four narrow bands in OMNBR models explained most (64% to 92%) of the variability in crop biophysical variables. The second part of the paper describes a rigorous search procedure to identify the best narrow band NDVI predictors of crop biophysical variables. Special narrow band lambda (*λ_1*) versus lambda (*λ_2*) plots of* R^2 *values illustrate the most effective wavelength combinations (*λ_1 *and* λ_2*) and bandwidths (*$\Delta\lambda_1$ *and* $\Delta\lambda_2$*) for predicting the biophysical quantities of each crop. The best of these two-band indices were further tested to see if soil adjustment or nonlinear fitting could improve their predictive accuracy. The best of the narrow band NDVI models explained 64% to 88% variability in different crop biophysical variables. A strong relationship with crop characteristics is located in specific narrow bands in the longer wavelength portion of the red (650 nm to 700 nm), with secondary clusters in the shorter wavelength portion of green (500 nm to 550 nm), in one particular section of the near-infrared (900 nm to 940 nm), and in the moisture sensitive near-infrared (centered at 982 nm). This study recommends a 12 narrow band sensor, in the 350 nm to 1,050 nm range of the spectrum, for optimum estimation of agricultural crop biophysical information.* ©*Elsevier Science Inc., 2000*

INTRODUCTION, RATIONALE, AND BACKGROUND

The spectral data from the current generation of earth-orbiting satellites carrying broad band sensors such as Landsat Thematic Mapper (TM), Le Systéme pour l'observation de la terre (SPOT) high resolution visible (HRV), and the Indian Remote Sensing (IRS) Linear Imaging Self-Scanning have limitations in providing accurate estimates of biophysical characteristics of agricultural crops (Fassnacht et al., 1997; Thenkabail et al. 1995; Wiegand et al. 1991; Wiegand and Richardson, 1990), natural vegetation (Friedl et al., 1994), and in quantifying other terrestrial ecosystem characteristics, such as soil characteristics; stress due to weeds, water, and nitrogen deficiencies or excess; crop phenology; and fallow, forest, and agricultural interactions (Moran et al., 1994; Running, 1989). These limitations have motivated

* Center for Earth Observation (CEO), Yale University

† International Center for Agricultural Research in the Dry Areas (ICARDA), Aleppo, Syria

Address correspondence to P. S. Thenkabail, Center for Earth Observation (CEO), Department of Geology and Geophysics, Kline Geology laboratory, P.O. Box 208109, 210 Whitney Avenue, Yale University, New Haven, CT 06520-8109, USA. E-mail: prasad.thenkabail@yale.edu

Received 19 February 1999; revised 15 June 1999.

REMOTE SENS. ENVIRON. 71:158–182 (2000)

655 Avenue of the Americas, New York, NY 10010

0034-4257/00/$–see front matter
PII S0034-4257(99)00067-X

the inclusion of hyperspectral sensors onboard the new generation of satellites planned by various governments and also by the United States private industry (e.g., see ASPRS, 1995; Stoney and Hughes, 1998). The upcoming narrow band hyperspectral sensors include: (1) Hyperion sensor with 220 spectral bands, each with 10 nm wide narrow bands onboard the National Atmospheric and Space Administration's (NASA) New Millennium Program's Earth Observer-1 (EO-1); (2) hyperspectral imaging spectrometer sensor with 105 spectral bands onboard Australian Resource Information Environmental Satellite-1; (3) Warfighter-1 with 200 channels onboard ORBVIEW-4 (a U.S. private industry satellite); and (4) moderate resolution imaging spectrometer (MODIS) with 36 channels (with 10 in visible, six in shortwave infrared or middle infrared, five in thermal infrared, and the rest beyond) onboard Terra (formerly EOS AM-1). The spectral range of these sensors will be 400 nm to 2500 nm. Apart from their high spectral resolution, Hyperion and the Australian sensors also have 30 m spatial resolution. Warfighter-1 will have eight meter resolution. However, MODIS has a much coarser spatial resolution, varying between 250 m and 1,000 m. All satellites are planned for launch either during the last quarter of 1999 or early 2000.

Recent literature has shown that the narrow bands may be crucial for providing additional information with significant improvements over broad bands in quantifying biophysical characteristics of agricultural crops. The hyperspectral data for studies reported in literature have been gathered using field spectroradiometers (Blackburn, 1998a; Carter, 1998; Elvidge and Chen, 1995; Shibayama and Akiyama, 1991; Curran et al., 1990), the Compact Airborne Spectrographic Imager (see Gong et al., 1995), and the NASA-designed Airborne Visible-Infrared Imaging spectrometer (AVIRIS, see Chen et al., 1998, Elvidge et al., 1993; Elvidge and Mouat, 1989). In the past three decades, the broad band vegetation indices (VIs) such as TM-derived NDVI have been widely used to quantify crop variables such as wet biomass (WBM), leaf area index (LAI), plant height, and grain yield (see, for example, Tucker, 1979; Wiegand et al., 1992; Thenkabail et al., 1995). These broad band indices (e.g., Lyon et al., 1998) use average spectral information over broad band widths (e.g., TM band 3 or red: 630–690 nm, and TM band 4 or near-infrared: 760–900 nm), resulting in loss of critical information available in specific narrow bands (e.g., Blackburn, 1998a). Also, the NIR and red-based indices are known to be heavily influenced by soil background at low vegetation cover (Elvidge and Lyon, 1985; Huete et al., 1985). Further improvement in indices is generally possible through use of spectral data from distinct narrow bands and, further, through corrections for soil background effects. These hyperspectral studies were conducted for rice yield (Shibayama and Akiyama, 1991), chlorophyll content of plants (Blackburn, 1998a, 1998b; Curran et al., 1990), coniferous forest LAI (Gong et al., 1995), pinyon pine canopy LAI (Elvidge and Chen, 1995), and photosynthesis and stomatal conductance in pine canopies (Carter, 1998). The soil-adjusted vegetation index and its numerous modifications (see Huete, 1988; Qi et al., 1994; Rondeaux et al., 1996; Lyon et al., 1998) further improve the performance of these indices through "adjustments" for soil background effects.

The indices discussed above involve two bands. According to Lawrence and Ripple (1998) and Gong et al. (1995), the use of two-band vegetation indices unnecessarily constrains the regression analysis. They argue that if one requires knowledge of an ecological variable (e.g., above-ground biomass or LAI), the researchers must ultimately analyze the relationship between the spectral index used and the ecological variable through a regression analysis. They and some others (e.g., Shibayama and Akiyama, 1991; Ripple, 1994) have shown that the piecewise multiple regression models performed on discrete narrow bands provide flexibility in choosing the bands that provide maximum information at a given period of crop growth. As the crop conditions vary due to factors such as management conditions, soil characteristics, climatic conditions, and cultural practices, different band combinations can be used (Shibayama and Akiyama, 1991; Shibayama et al., 1993).

Based on the above background, the main goal of this research is to evaluate the performance of various types of hyperspectral vegetation indices in characterizing agricultural crop biophysical variables. The final goal is to determine and recommend an optimal number of hyperspectral bands, their centers and widths, in the visible and NIR portion of the spectrum (350–1,050 nm) required to best study agricultural crops, thus reducing the redundancy in hyperspectral data. A rigorous and exhaustive approach is adopted in computing and evaluating hyperspectral indices. Crop variables used are LAI, WBM, grain yield, and plant height, which are the best indicators of crop growth and yield (see Bartlett et al., 1988; Wiegand and Richardson, 1990; Shibayama et al., 1993; Thenkabail et al., 1995; Fassnacht et al., 1997). Biophysical quantities are based on data from five agricultural crops, each with four crop variables.

STUDY AREA

The study area is located about 35 km southwest of Aleppo, Syria. Measurements were taken in farm fields that surround this area with the points falling within the area encompassed by upper left: 36°26′ 29.5836″ N, 36°35′ 24.3816″ E; lower right: 34°57′ 46.3428″ N, 37°43′ 47.3736″ E. The Aleppo area is characterized by Mediterranean climate: hot and dry summers and cool and wet winters. The annual rainfall varies from 300 mm to 350 mm. This climate pattern occurs in several loca-

tions in the 30–40-degree latitude belts in both hemispheres. The largest single contiguous area experiencing this climate is in the Mediterranean basin covering parts of West Asia, North Africa, and Southern Europe. Hence a study conducted in such a representative area (Aleppo) has applications across many other Mediterranean regions falling within similar climatic, vegetation, and agricultural patterns. The overall study area had four soil types: very fine clayey chromic calcixerert (the Jindiress region), very fine clayey calcixerollic xerochrept (Tel Hadya), clayey calcixerollic xerochrept (Breda), and clayey mixed thermic calcic gypsiorthid (Ghrerife) (Ryan et al., 1997). During summer, 10% to 20% of the farms in the study area are irrigated from deep wells (recharged by aquifers), or by canal irrigation from the Euphrates River. Otherwise most of cultivation is rain-fed during the winter and spring (November–April).

METHODS: COMPUTATION OF NARROW BAND INDICES AND LABORATORY PROCEDURES

Spectral and biophysical data were gathered for five irrigated summer (July–October) crops. All data were collected during a 15-day field campaign in late August and early September 1997. A 512 channel spectroradiometer with a range from 331.8 nm to 1,063.95 nm, manufactured by Analytical Spectral Devices™ (FieldSPEC, 1997), was used to gather spectral data of crops and soils. Due to severe noise in the ends of the spectrum, only the data gathered in 350 nm through 1,050 nm was used, reducing the number of spectral channels to 490. The band centers were rounded off to nearest whole number (e.g., 549.86 nm as 550 nm). The spectroradiometer unit consisted of a main spectrometer, a personal computer, fiber optic cable, a pistol grip, and different field of view (FOV) cones. Inside the spectrometer instrument, light is projected from the fiber optics onto a holographic diffraction grating where wavelength components are separated and reflected for independent collection by the detector(s) (FieldSPEC, 1997). Five major crops were identified for spectral and crop biophysical measurements. The major crops during this summer period were: cotton (*Gossypium*), potato (*Solanum erianthum*), soybeans (*Glycine max*), corn (*Zea mays*), and sunflower (*Helianthus*). These farms were on four distinct soil zones. Hence the soil types, color, and transformation (tilled, untilled, fallow) of the soils were noted at each location. Spectral reflectance data and quantitative and qualitative data on crops and soils were obtained from 194 locations spread across the study area. The sample distribution was: cotton (73 sample locations), potato (25 sample locations), soybeans (27 sample locations), corn (17 sample locations), sunflower (9 sample locations), and topsoil (43 sample locations) (Fig. 1). The mean spectral plots of these crops are shown in Fig. 1a through d, taking their distinctive growth stages. These growth phases were (Table 1): early vegetative (potato, soybeans), late vegetative (soybeans, corn), critical (cotton, soybeans, corn), and yielding/maturing (cotton). Plots of the first-order derivative spectra (not presented here) will show the regions of change and the degree of change in spectral reflectivity with change in wavelength across the spectrum. At each site, 3 to 10 reflectance measurements were consistently taken along a transect, with a nadir view from a height of 1.2 m for cotton, potato, and soybeans, using a 18° FOV. This resulted in viewing an area of 1,134 cm^2 at the ground level. Typical transact was 30 m to 100 m in length with one spectra at every 10 m interval. For corn and sunflower the viewing height was 1.8 m. Spectroradiometer data of crops were analyzed using softwares PORTSPEC™ and VNIR™ supplied by the manufacturer of the instrument (Analytical Spectral Devices™), and Statistical Analysis System (SAS) version 6.12 (SAS, 1997a, 1997b). The target reflectance is the ratio of energy reflected off the target (e.g., crops) to energy incident on the target (measured using a $BaSO_4$ white reference). Since the dark current varies with time and temperature, it was gathered for each integration time (virtually for each new reading). Thus [see Eq. (1)],

$$\text{Reflectance (\%)} = \frac{(\text{target-dark current})}{(\text{reference-dark current})} \cdot 100 \quad (1)$$

Three distinct types of narrow band indices were computed using 490 spectral channels of percentage reflectance data from the spectroradiometer. The hyperspectral indices computed were (see Table 2): (1) all possible two-band combination indices involving the 490 narrow bands; (2) stepwise linear regression indices involving 490 narrow bands; and (3) the soil-adjusted narrow band indices.

The performance of these indices in establishing crop characteristics (Table 1) were then evaluated and compared with the well-known reference Landsat TM broad band indices. At each farm, a representative area of 1 m^2 was chosen for all measurements. At each sample site, two to four sets of reflectance measurements were taken for one representative plant. The same plant sample above the ground was taken for laboratory analysis. Above-ground plant height (mm), number of plants in 1 m^2 area, and number of rows was recorded. Observations were made on the crop growth stage (Fig. 1) and crop condition. Where farmers were available, planting dates were recorded that were used in conjunction with crop growth stages. A digital photograph was taken at each site to further supplement the above quantitative and qualitative observations. Digital photographs provided valuable additional information on each site, for example, in identifying cotton fields that are nearing harvest versus

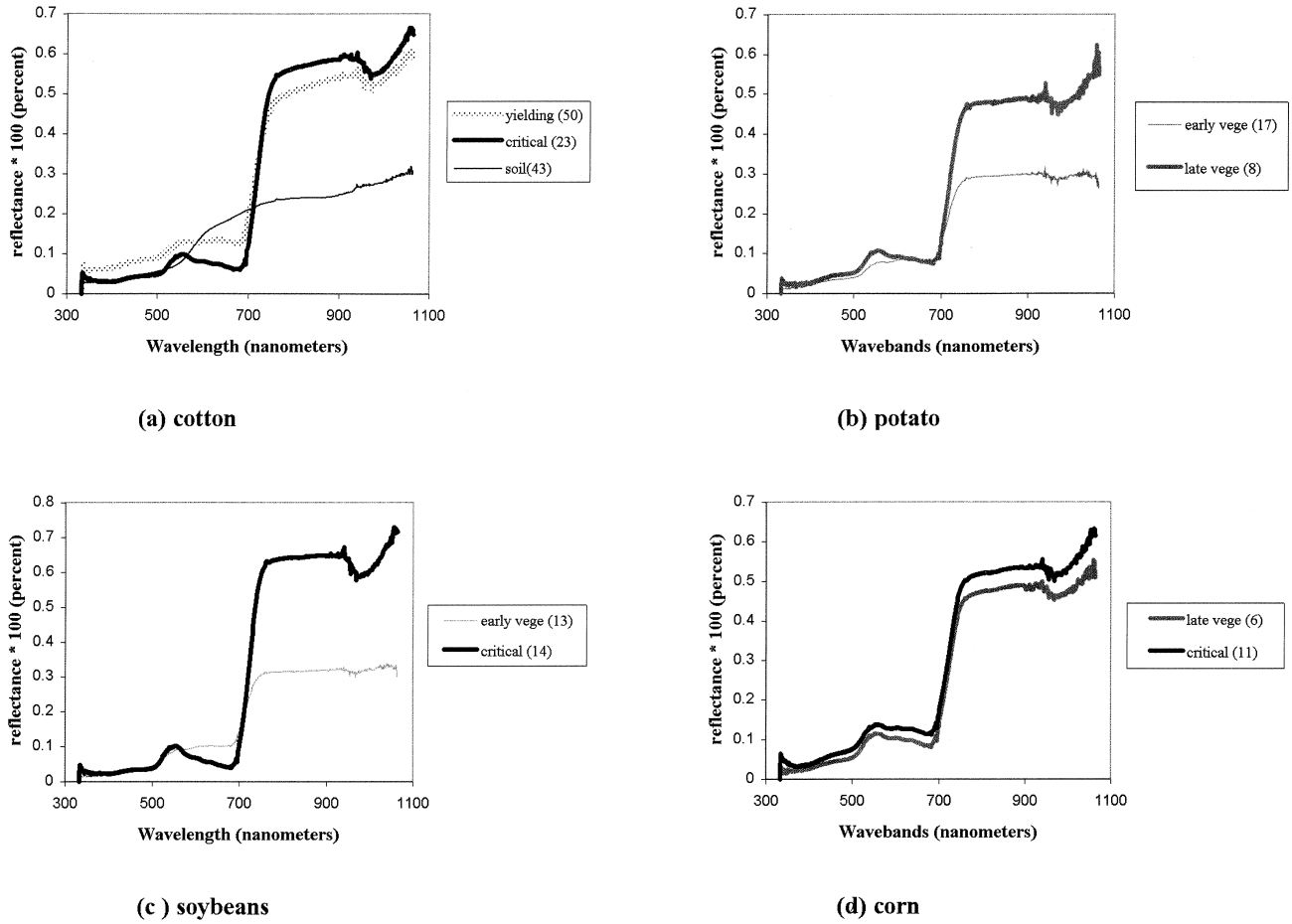

Figure 1. Spectral reflectance characteristics of different crops at distinct growth phases. Sample sizes are shown inside the legend brackets of each crop.

those that are in critical/flowering stages (e.g., Figs. 1a and b). Photographs also helped in identifying gross mistakes, if any, in plant density calculations and crop condition rating. Global Positioning System locations were noted in geographic coordinates (latitude/longitude in degree, minutes, seconds) and in universal transverse mercator (in meters) were recorded. In the laboratory, plant samples were analysed for leaf area (m^2), wet weight (kg), and (in the case of cotton) yields (kg lint/ha) (Table 1). Leaf area was obtained by running the leaves over a LI-COR 3100 leaf area meter. The leaf area obtained from one representative plant is multiplied by the number of plants in 1 m^2 area to obtain LAI (m^2/m^2). Plants were cut and weighed on a simple weighing machine. This weight was multiplied by number of plants in 1 m^2 to obtain biomass (kg/m^2). LAI and WBM and plant height measurement were made for all crops (Table 1). Yield was also obtained for cotton. For this purpose cotton bolls were counted and converted to kg lint per hectare (kg lint/ha) using 600 bolls per 1 kg lint. Yields were not gathered for other crops. The mean reflectance values obtained for these soils were plotted for various narrow bands λ_1 and λ_2, and fitted using an equation of type: NIR=a·red+b. The slopes (a) and intercepts (b) obtained from the soil lines were used in the soil adjusted vegetation indices (e.g., narrow band TSAVI). For further details on methods and procedures refer to Thenkabail et al. (1999).

RESULTS AND DISCUSSION

The relationships between the four biophysical variables of five crops and four types of reflectance indices are discussed below. Of these, the first index type is broad band and the others are narrow band. These indices are:

- broad band TM NDVI (as our reference index);
- OMNBR reflectance models;
- two-band NDVI type indices involving all possible combinations of 490 narrow bands; and
- narrow band soil-adjusted vegetation indices.

An overwhelming proportion of the Hyperspectral index models indicated that the best relationships were obtained using LAI or biomass of different crops. The relationships with crop height, yield, and canopy cover also provided several high R^2 values, but performed poorer

Table 1. General Crop Characteristics, Growth Stages and Crop Type Discrimination

	Ground-Measured Crop Variables					*Spectral Vegetation Indices*				
Crop Growth Stage	*WBM (kg/m^2)*	*LAI (m^2/m^2)*	*plant height (mm)*	*Yield (kg lint/ha)*	*Canopy cover (percentage)*	*Broad band NDVI (TM4 and TM3) NIR/red (broad band-TM)*	*Broad band GVI (TM1, TM2, TM3, and TM4) four-band index*	*Narrow band NDVI1 (0.550 μm and 0.468 μm) green/blue*	*Narrow band NDVI2 (0.550 μm and 0.682 μm) green/red*	*Narrow band NDVI3 (0.920 μm and 0.696 μm) NIR/red*
Corn critical (11)	2.70	1.50	1471	N/A	100	0.67	44.67	*0.39*	*0.13*	*0.66*
Corn late vegetative (6)	2.23	2.06	1105	N/A	85	0.67	38.37	*0.45*	*0.27*	*0.73*
Corn (17) all fields	2.53	1.70	1342	N/A	95	0.67	42.45	0.41	0.18	0.68
Cotton critical (23)	2.58	1.38	858	1282	95	*0.78*	*49.12*	*0.39*	*0.24*	*0.81*
Cotton yielding (50)	1.53	0.70	738	1056	85	*0.59*	*41.73*	*0.25*	*0.045*	*0.65*
Cotton (73) all fields	1.86	0.91	776	1127	88	0.66	44.06	0.29	0.11	0.70
Potato early vegetative (17)	0.75	0.34	269	N/A	18	*0.54*	*23.65*	0.35	*−0.004*	0.55
Potato late vegetative (8)	1.63	0.66	363	N/A	35	*0.70*	*40.40*	0.36	*0.16*	*0.72*
Potato (25) all fields	1.03	0.44	299	N/A	23	0.59	29.01	0.36	0.05	0.60
Soybean critical (14)	2.56	3.17	558	N/A	90	*0.84*	*54.52*	*0.50*	*0.46*	*0.88*
Soybean vegetative (13)	0.40	0.49	204	N/A	40	*0.49*	*24.55*	*0.41*	*−0.033*	*0.54*
Soybeans (27) all fields	1.52	1.84	388	N/A	66	0.67	40.09	0.46	0.22	0.72
Sunflower flowering (9)	3.75	2.07	1022	N/A	100	0.73	47.14	0.39	0.33	0.79
Distinguishable crops						Corn-pot Cot-pot Pot-sflower	Corn-pot Cot-pot Pot-sbeans Pot-sflower	Corn-cot Cot-pot Cot-sbeans Cot-sflower Pot-sbeans	Corn-cot Corn-pot Corn-sflower Cot-pot Cot-sbeans Cot-sflower Pot-sbeans Pot-sflower Sbeans-sflower	Corn-pot Corn-sflower Cot-pot Cot-sflower Pot-sbeans Pot-sflower

Broad band indices are for Landsat TM bands. NDVI1, NDVI2, and NDVI3 are narrow band indices. NDVI1 has band centers at 0.550 μm (green) and 0.468 μm (blue). GVI=green vegetation index of first four TM bands. This is computed using the principal analysis component. See Jackson (1983), Kauth and Thomas (1977), Crist and Cicone (1984), and Wheeler and Misra (1976). The GVI equation is: GVI=0.056710·TM1+0.008573·TM2−0.423309·TM3+0.904168·TM4. Significant differences at 0.10 level or higher for mean vegetation index values between any two crop growth stages of a crop are set in italic. pot=potato, cot=cotton, sbeans=soybeans, sflower=sunflower.

Table 2. Indices Used in This Study

Vegetation Index Group	*Vegetation Index Name*	*Abbreviation*	*Definition*	*Reference*
1. Broad band: Thematic Mapper	Normalized difference vegetation index (broad band)	Broad band NDVI	$\frac{\text{NIR}-\text{red}}{\text{NIR}+\text{red}}$ red: 630–690 nm, NIR: 760–900 nm of Landsat TM sensor	Rouse et al. (1973); Jackson (1983)
2. Narrow band: multiple linear regression	Optimum multiple narrow band reflectivity (narrow band)	OMNBR	$B_i=\sum_{j=1}^{N} a_{ij}R_j$ where B=crop variable i, R=reflectance in bands j (j=1 to N with N=490); a=the coefficient for reflectance in band j for ith variable. Using MAXR algorithm in SAS (1997a), the best 1, 2, 4, n-variable models are calculated for each crop variable with equations of the form: $\alpha+a_1\cdot\text{NB}_1$ $a+a_1\cdot\text{NB}_1+a_2\cdot\text{NB}_2$ $a+a_1\cdot\text{NB}_1+a_2\cdot\text{NB}_2+a_3\cdot\text{NB}_3+a_4\cdot\text{NB}_4$ and so on. Where NB=narrow-band and a=intercept. The model will use hyperspectral bands 1 to 490 (each band of 1.43 nm wide and spread over 350–1050 nm) and pick a single band providing highest R^2 value, then finds the two-band combination that provides highest R^2 value and so on. a=slope or gain of the soil line; b=intercept or offset of the soil line obtained by plotting NIR and red bands. Note that these lines are different for the broad bands and narrow bands.	This paper (see Table 1)
3. Narrow band: normalized difference between all possible two-band combinations of λ_1 and λ_2 (λ_1=1 to 490 bands, λ_2=1 to 490 bands)	Normalized difference vegetation index (narrow band)	Narrow band NDVI	narrow band $\text{NDVI}_{ij}=\frac{(R_j-R_i)}{(R_j+R_i)}$ where i,j=1, N is reflectance (percent) of narrow bands with N=narrow bands=490 (each band of 1.43 nm wide and spread over 350–1050 nm); R=reflectance of narrow bands	This paper (see Fig. 4 and Fig. 5)
4. Narrow band: soil adjusted	Transformed soil-adjusted vegetation index (narrow band)	Narrow band TSAVI	$\frac{a\cdot(\text{NIR}-a\cdot\text{red}-b)}{(\text{red}+a\cdot\text{NIR}-a\cdot b)}$; a=slope and b=intercept of soil lines	Baret et al. (1989)

than LAI and biomass models. Hence, the main focus of the results presented in this paper will be for LAI and biomass. Limited results are also presented for other relatively less significant crop variables.

However, the study begins with a direct evaluation of the correlation between the single band reflectance with biophysical quantities. It was determined during a preliminary sensitivity analysis that the vegetation indices computed for a wide range of the existing sensors such as Landsat MSS, Landsat TM, SPOT HRV, NOAA AVHRR, and IRS-1C, using simulated data for crops from a spectroradiometer, were highly correlated (R^2=0.95 or higher). Hence computing vegetation indices for any one of these sensors will provide nearly the same information as similar indices computed for other sensors. Elvidge and Chen (1995) determined that the relatively narrower bands of TM and MSS sensors showed only slight improvements over broader bands from sensors such as AVHRR. Therefore, the TM NDVI (see Table 2) was the only broad band index computed and reported throughout this paper. The discrete 1.43 nm wide narrow band reflectance data obtained using the spectroradiometer were averaged over the spectral bands 760 nm to 900 nm (for TM band 4) and 630 to 690 nm (for TM band 3) to obtain broad band NDVI for each data point.

Single Narrow Band Reflectance Relationships with Crop Variables

As a first step, reflectance in the 490 individual narrow bands was correlated with crop biophysical variables: WBM and LAI of all the five crops (Fig. 2). Maximum negative correlation coefficients (r) in the red band portion were mostly centered around 680 nm. This is a region of high chlorophyll absorption in green vegetation. The maximum negative r values for relationships between reflectance and WBM were (Fig. 2a) at 682 nm for cotton (r=−0.75), potato (−0.47), soybeans (−0.72), and corn (−0.41) (Fig. 2a). For sunflower it was centered at 625 nm (r=−0.58). There were similar trends with LAI (Fig. 2b). Around 700 nm, the amount of energy reflected off green vegetation begins to increase. The wavelength portion 700 nm to 780 nm has the highest change in reflectance per unit change in wavelength in all of the visible and NIR portion of the spectrum, reaching a peak around 780 nm (see Fig. 1). The r values change dramatically from negative around 682 nm to positive around 740 nm for biomass (Fig. 2a) and LAI (Fig. 2b) for all crops. In the 740 nm to 875 nm portion of the spectrum, r values for WBM and LAI are high and nearly constant. Beyond 875 nm, other crop specific relationships are seen. For example, maximum r values for cotton crop reflectance with: (1) WBM was 0.55 at 910 nm (Fig. 2a), and (2) LAI was 0.51, also at 910 nm (Fig. 2b). Maximum positive r values between reflectance and WBM were (Fig. 2a) 0.55 at 910 nm for cotton, 0.51 at 910 nm for potato, 0.83 at 825 nm for soybeans, 0.32 at 940 nm for corn, and 0.53 at 868 nm for sunflower. Similarly, maximum positive r values between reflectance and LAI were (Fig. 2b) 0.51 at 910 nm for cotton, 0.59 at 1025 nm for potato, 0.65 at 854 nm for soybeans, 0.17 at 768 nm for corn, and 0.46 at 882 nm for sunflower. The 940–1,040 nm moisture sensitive "trough" in percent reflectance spectra becomes more significant with increasing biomass and crop moisture (Penuelas et al., 1993). The trough minima were near 982 nm for most crops (see Figs. 1a–d). In contrast to the NIR shoulder (780 nm to 900 nm), in which spectral reflectance changes only marginally for all crops (except cotton and corn), the visible portion of the spectrum (400–700 nm) is highly sensitive in different discrete portions in blue, green, and red, as evident in Fig. 1. This characteristic resulted in a rapidly changing correlation coefficient between crop biophysical variables (WBM and LAI) and spectral reflectance for a given crop in 400–700 nm compared to the relatively uniform r values in 780–900 nm (Fig. 2).

OMNBR Reflectance Relationships with Crop Variables

The OMNBR reflectance indices (see Table 2), were related to crop biophysical variables through stepwise linear regression analysis. The dependent variables (B_i) in the model are crop variables and independent variables are reflectances (R_j) in the 490 discrete narrow bands. Of several statistical methods available to run piecewise linear regression models, the stepwise MAXR procedure (SAS, 1997a, 1997b) is considered the best and hence is used in this study. Using the MAXR procedure, the model providing the highest R^2 value for one-, two-, and four-variable OMNBR models were determined for developing relationships with WBM, LAI, and plant height of four crops (cotton, potato, soybeans, and corn), as well as yield of cotton crop (Table 3). In 10 of 13 biophysical variables, the first four narrow band variables explained 76% or above variability (Table 3). This is nearly the same percentage of variability explained when the ratio of the number of independent variables or number of bands (M) to that of the total number of field samples (N) for that variable is between 0.15 and 0.20 in different crop variables (see Fig. 3). As M approaches N, the R^2 value approaches 1. Beyond M/N of 0.15 to 0.20 (see Fig. 3), there were only small increases (often statistically insignificant) with addition of another variable. This feature has been illustrated in Fig. 3 for the relationships between narrow bands and LAI of four crops by comparing them with idealised random (RAND in Fig. 3) plot, which shows the nature of the curve when the sample sizes are large (350 in this case). For each crop, the R^2 values were statistically significant for the one-variable

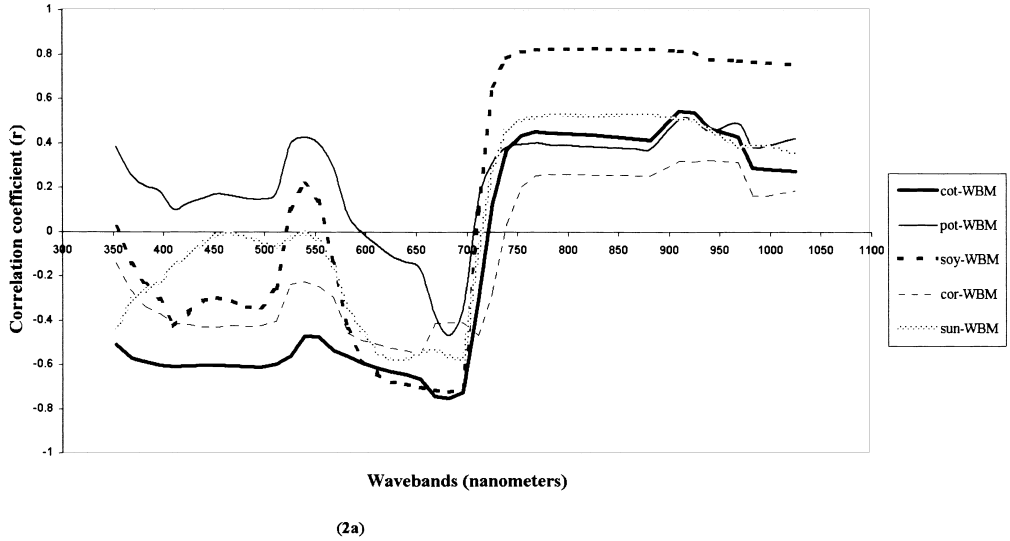

(2a)

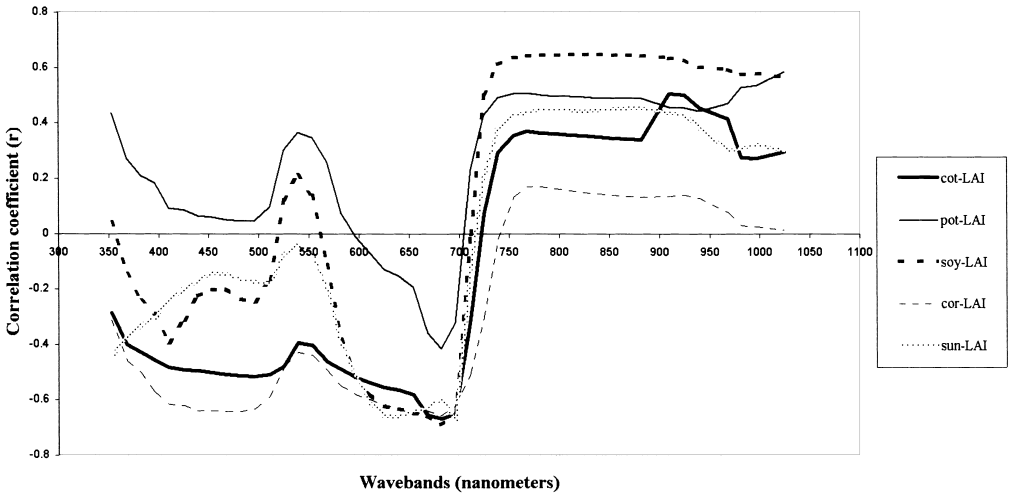

(2b)

Figure 2. Correlation coefficients (*r*) between spectral reflectance in the 512 discrete channels and biophysical variables of the five crops for (a) WBM and (b) LAI.

models and increased significantly with the addition of a second, third, and, at times, the fourth variable (Fig. 3 and Table 3). Four-variable models explained 64% to 92% variability in crop biophysical variables, significantly higher than 53% to 81% by two-variable models, and 18% to 69% by one-variable models (Table 3). Beyond the fourth variable, the increases with addition of each variable is small and statistically insignificant. A quality factor ($Q=R^2_{crop}/R^2_{rand}$) demonstrates that the statistical significance of the extra information decreases as more channels are added. For example, Q for the first five values of cotton crop were 3.38, 2.50, 1.93, 1.89, and 1.81. The first two-variables explain most of the variability. Any increase in R^2 beyond $M/N=0.15$–0.20 is an mathematical artefact arising from limited sample size compared to the number of channels in a hyperspectral sensor. (Note: for corn with only 17 samples, N, even a four-band, M, index exceeds the threshold M/N value of 0.20.) These results compare well with Blackburn (1998a), who mentions that there is a likelihood of the multiple narrow band models being "over-fit" and hence the relationships need to be validated using independent datasets.

The first two bands, typically, constitute a red and NIR, a red and a green or a red-edge and a NIR band combinations (see bands of two-variable models in Table 3). In four-variable models the bands that occur most clustered in the longer wavelength portion of red (651 nm to 700 nm), moisture-sensitive NIR (951 nm to 1000 nm), shorter wavelength portion of green (501 nm to 550 nm), and longer wavelength portion of NIR (900 nm to 940 nm). This result suggests the fact that the optimal information on crops is not necessarily concentrated in the red and NIR wavelengths. The waveband combinations providing optimal information are dependent on a

Table 3. Optimum Multiband predictors

Crop Type (Sample Size)	*Dependent Crop Variable*	*Best One-Variable Model OMNBR*		*Best Two-Variable Model OMNBR*		*Best Four-Variable Model OMNBR*		*Best R^2 Value for Two-Band Normalized Difference Vegetation Index Models (Results from Table 4)*		*Percent Increase in Four Best Variable Model*	
		Band centers (nm) (Independent Variable)	R^2	*Band Centers (nm) (Independent Variables)*	R^2	*Band Centers (nm) (Independent Variables)*	R^2	*Broad Band NDVI Model* R^2	*Narrow Band NDVI Model* R^2	*Broad Band NDVI*	*Narrow Band NDVI*
1. Cotton (73) except for yield for which the sample size is 49	WBM	682	0.56	682,910	0.75	368,668,925,968	**0.79**	0.76	**0.79**	+3	0
	LAI	682	0.44	682,910	0.60	353,682,925,968	**0.70**	0.61	0.66	+11	+4
	Plant height	910	0.40	682,925	0.53	668,696,910,982	**0.64**	0.41	0.52	+23	+10
	yield	954	0.52	696,968	0.73	525,582,668,968	**0.77**	0.54	0.64	+23	+13
2. Potato (25)	WBM	910	0.26	711,954	0.68	511,682,711,940	**0.80**	0.67	0.76	+23	+4
	LAI	1025	0.34	668,1025	0.67	525,568,682,997	0.80	0.78	**0.88**	+2	−8
	Plant height	910	0.31	668,910	0.60	425,539,568,668	**0.83**	0.68	0.77	+15	+6
3. Soybeans (27)	WBM	825	0.68	725,811	0.76	353,754,811,825	0.81	0.79	**0.84**	+12	−3
	LAI	682	0.47	668,682	0.61	668,682,811,954	0.76	0.72	**0.80**	+4	−4
	Plant height	825	0.69	739,811	0.81	525,739,754,982	**0.92**	0.75	0.78	+17	+13
4. Corn (17)	WBM	654	0.30	511,654	0.69	439,511,625,954	**0.78**	0.59	0.71	+19	+7
	LAI	682	0.43	482,982	0.60	410,496,511,1025	0.78	0.70	**0.86**	+9	−8
	Plant height	1025	0.18	725,1025	0.39	525,568,725,1025	**0.66**	0.26	0.31	+40	+38

Piecewise OMNBR models were obtained using MAXR algorithm in SAS (1997a and 1997b). The model with highest R^2 between OMNBR (four-variable), narrow band NDVI and broad band NDVI is shown in bold. Bandwidths are 1.43 nm wide for each band center. Band centers in fraction were rounded off to nearest whole number (e.g., 549.86 nm as 550 nm.

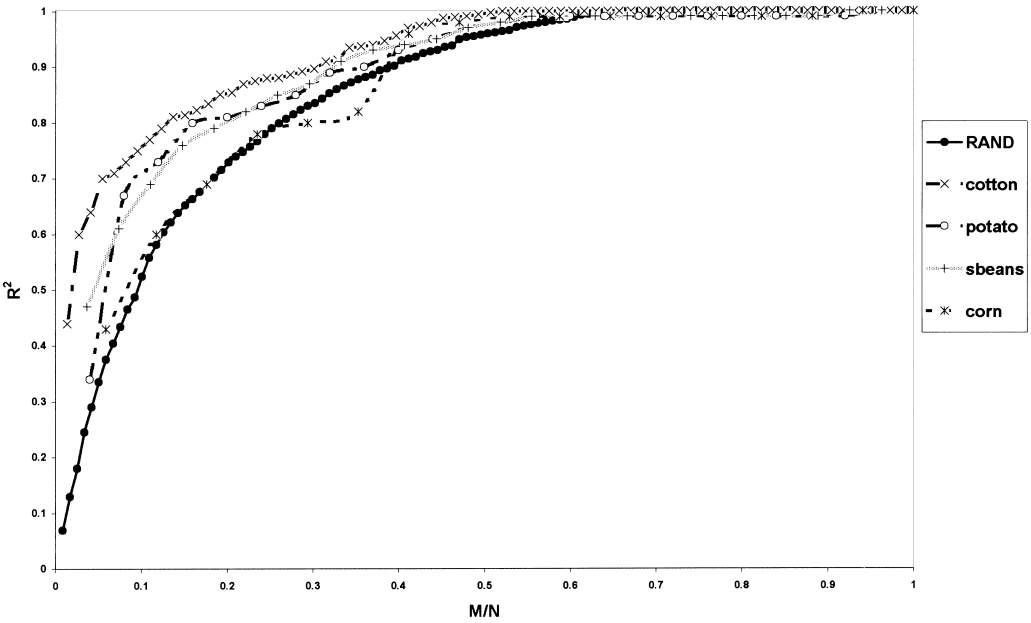

Figure 3. Plot of the ratio *M/N* versus R^2 value.

host of variables, such as crop growth stage, crop condition, and cultural practices. An interesting result in Table 3 is the frequent appearance of narrow bands from the visible portion (400 nm to 700 nm) apart from the longer wavelength portion of NIR and the moisture-sensitive NIR. The visible spectrum is very sensitive to loss of chlorophyll, browning, ripening, and senescing (Idso et al., 1980), variations in carotenoid (Blackburn, 1998b; Tucker, 1977) and soil background effects. The visible spectrum is highly sensitive to crop senescence rates and is generally an excellent predictor of grain yield (Idso et al., 1980). This study showed that the most sensitive portion of bands to predict senescing cotton (sample size 50) yield were predominantly in the visible red narrow bands (centered at 696 nm or 668 nm) and moisture-sensitive NIR (968 nm and/or 954 nm) (see these bands in one-variable, and/or two-variable, and/or four-variable models in Table 3).

Narrow Band NDVI Relationships with Crop Variables

The availability of hyperspectral data in 490 (N) discrete narrow bands allowed computation of $N \times N = 240{,}100$ narrow band NDVIs for any one crop variable (Table 2). Regression coefficients R^2 between all possible two-band narrow band vegetation indices and crop biophysical variables were determined. The result of this comprehensive analysis is illustrated in contour plots of the R^2 values, for each λ_1 and λ_2 pair, in Figs. 4 and 5. It suffices to display the matrix only below (or above) the diagonal of the matrix as the R^2 (λ_1 and λ_2) values are symmetrical. Further, in both these figures, only R^2 values above 0.4 are plotted for clarity. Similar contour plots (too numerous to be presented here) were created for all the other biophysical variables of each crop.

Based on the above results, band centers (λ_1 and λ_2) and band widths ($\Delta\lambda_1$ and $\Delta\lambda_2$) that combine to form the best seven indices (ranked based on R^2 values) were determined for WBM and LAI of cotton, potato, soybeans, corn, and for the pooled data of all crops (Table 4). The band centers and their widths are identified for the LAI, WBM models of each crop variable. This can be determined through λ_1 and λ_2 contour plots of R^2 values (Figs. 4 and 5). We determined that a contour interval of 0.05 for R^2 values provide a reasonable and statistically sound approach of arriving at band centers and band widths. Smaller contour intervals result in several more gradients of R^2 values, providing other band centers and band widths. These can be too numerous and often provide no significant statistical difference between two discrete contour intervals. For example, the index that has highest correlation for cotton WBM has band centers (λ_1 and λ_2) and bandwidth ($\Delta\lambda_1$, and $\Delta\lambda_2$) extracted from the contour plot range of 0.70 to 0.75 (highest R^2 value range) in the lower diagonal portion of Fig. 4. The band centers and bandwidths are (Fig. 4): $\lambda_1 = 682$ nm ($\Delta\lambda_1 = 28$ nm), and $\lambda_2 = 918$ nm ($\Delta\lambda_2 = 20$ nm). These band centers and widths are then tabulated in Table 4. The same range (0.70 to 0.75) of contour intervals can be split into distinctive groups of smaller intervals such as 0.70 to 0.72, 0.73 to 0.74, and >0.74. Then it is possible to derive band centers (λ_1 and λ_2) and bandwidths ($\Delta\lambda_1$ and $\Delta\lambda_2$) to each one of these smaller intervals. However, the significance of the band centers and bandwidths from the small intervals of R^2 values, such as between 0.70 to 0.72 and 0.73 to 0.74, is limited since these R^2 values did not

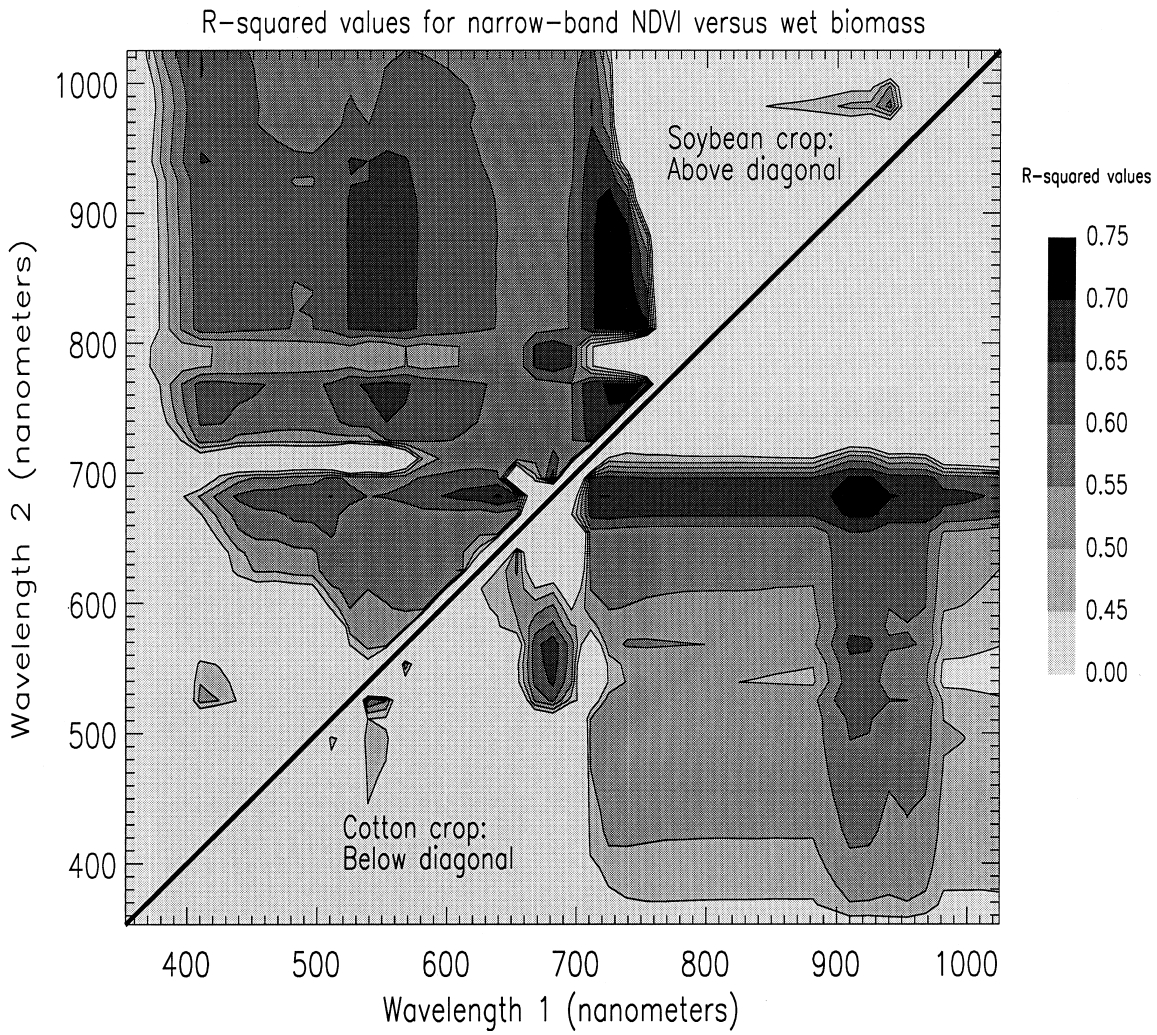

Figure 4. Contour plot showing the correlation (R^2) between WBM and narrow band NDVI values calculated for 490 narrow bands spread across λ_1 (350 nm to 1050 nm) and λ_2 (350 nm to 1050 nm). The different areas of "bulls-eye" are the regions with high R^2 values, which were ranked and from which band centers (λ_1 and λ_2) and band widths ($\Delta\lambda_1$ and $\Delta\lambda_2$) were calculated for the seven best indices of each crop variable, as in Table 5.

have significant statistical difference or were statistically different only at 0.10 level or higher. Therefore, the λ_1 and λ_2 spectral band combinations obtained from the distinctive contour intervals of 0.05 were considered a reasonable and statistically sound approach. The second best index (index with second highest correlation) is then selected from the contour plot region with R^2 value range of 0.65 to 0.70. Following a similar procedure, band centers and bandwidths of the seven best indices for a particular crop variable is determined (Table 4). Similar procedure is adopted for determining λ_1, λ_2 , $\Delta\lambda_1$, and $\Delta\lambda_2$ for indices of other crop variables and for the pooled data of all crops (Table 4). When visually inspecting the contour plots of R^2 values, it must be noted that more precise bandwidths are possible with a smaller range of contour interval plots of R^2 values than shown in Fig. 4 (which has a 0.05 R^2 value contour interval). An evaluation of these results for various crop variables show a remarkably strong relationships centered in the longer portion of red, 650 nm to 700 nm, a particular portion of NIR, 900 nm to 940 nm, and shorter portion of the green band, 500 nm to 550 nm (see specific narrow band centers and their widths in Table 4 and the clusters in Fig. 6). For the precise R^2 values, visually scan through 490 (N) by 490 (N) matrix of R^2 values. Identify the λ_1 and λ_2 band centers having highest R^2 value. This is the band center for the index, which has highest correlation. Observe the R^2 values in the immediate vicinity of these band centers (λ_1 and λ_2). Often the R^2 values remain the same or nearly the same for a few narrow bands in immediate vicinity of λ_1 and λ_2. This range of similar or near-similar spectral response to a crop variable will con-

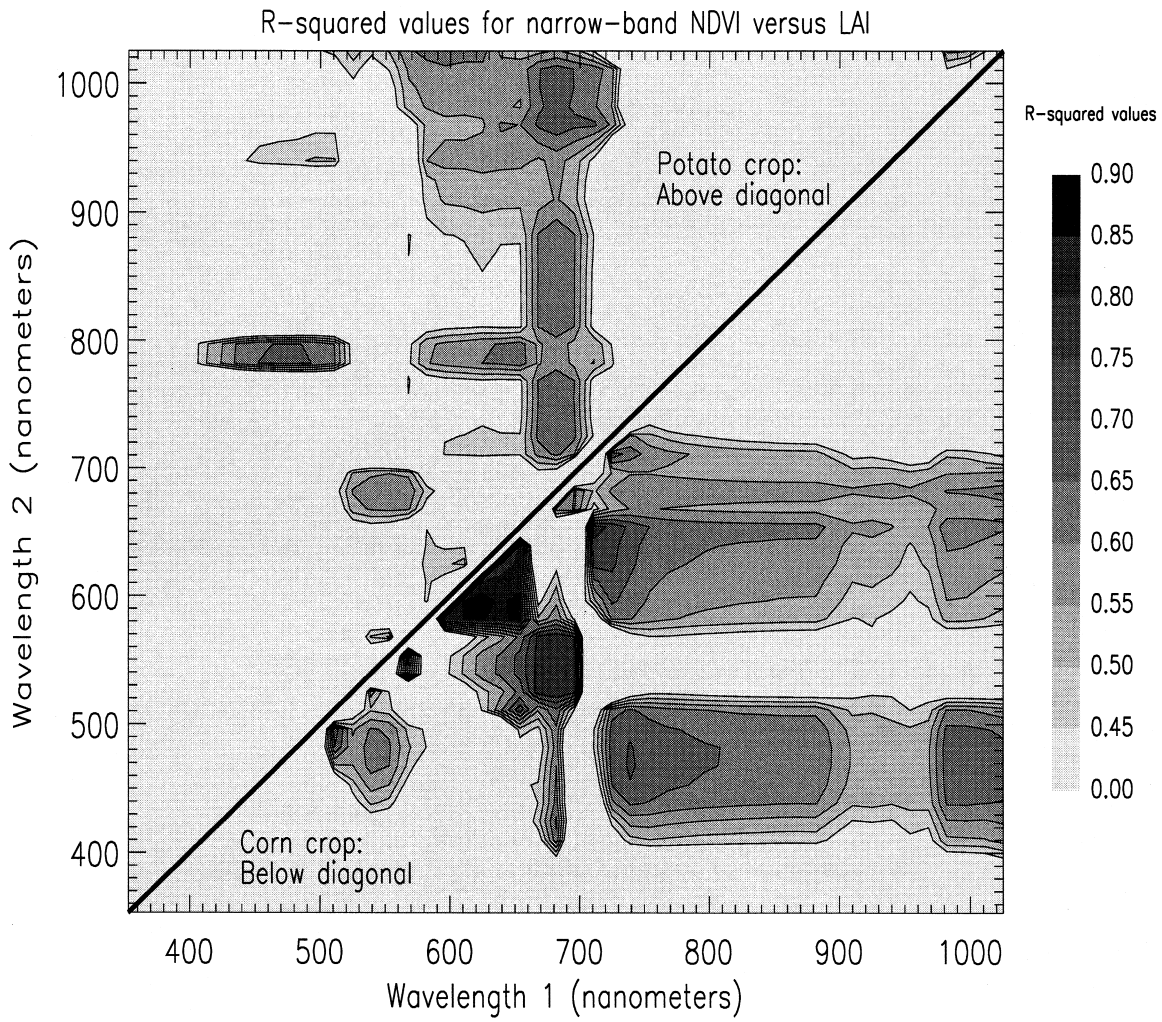

Figure 5. Contour plot showing the correlation (R^2) between LAI and narrow band NDVI values calculated for 490 narrow bands spread across λ_1 (350 nm to 1050 nm) and λ_2 (350 nm to 1050 nm). The different areas of "bulls-eye" are the regions with high R^2 values, which were ranked and from which band centers (λ_1 and λ_2) and band widths ($\Delta\lambda_1$ and $\Delta\lambda_2$) were calculated for the seven best indices of each crop variable, as in Table 5.

stitute the bandwidth. Bandwidths can also be assessed by systematically increasing bandwidth centered over a wavelength (at 1 nm or 2 nm steps) or using prespecified bandwidths. However, the approach adopted in this paper is more comprehensive when compared to these approaches.

Narrow Band Nonlinear Model Relationships with Crop Variables

Figures 4 and 5 depict R^2 values for linear relationships between crop biophysical variables and hyperspectral indices. However, most relationships between crop biophysical variables and spectral indices are nonlinear. It was noticed in this study that overwhelming proportions of the best nonlinear models were exponential (e.g., Fig. 7). The band centers (λ_1 and λ_2) and band widths ($\Delta\lambda_1$ and $\Delta\lambda_2$) determined for the seven best linear models (Table 4) were used for computing nonlinear exponential models. The R^2 values for the seven best linear and nonlinear exponential narrow band vegetation index models were computed and listed for each biophysical variable (Table 5). The best hyperspectral models for WBM explained 79% variability for cotton, 76% variability for potato, 84% variability for soybeans, 71% variability for corn, and 59% variability for all crops Table 5). Similarly, the best LAI models explained 66% variability for cotton, 88% variability for potato, 80% variability for soybeans, 86% variability for corn, and 65% variability for all crops. Except in three cases, nonlinear models performed substantially better than the linear models. However, in three cases (corn WBM, corn LAI, and cotton yield) linear models performed better than the nonlinear models.

Table 4. Seven best NDVIs. Band Centers (λ_1 and λ_2) and Band Widths ($\Delta\lambda_1$ and $\Delta\lambda_2$) in nm for the Linear Narrow band NDVI Models for the Different Crop Variables

Crop (Sample Size)	*Crop Variable*	*Band Center and Width (nm)*	*Band Centers (λ_1 and λ_2) and Band Widths ($\Delta\lambda_1$ and $\Delta\lambda_2$) for Two-Band Vegetation Indices*						
			Index 1 (nm)	*Index 2 (nm)*	*Index 3 (nm)*	*Index 4 (nm)*	*Index 5 (nm)*	*Index 6 (nm)*	*Index 7 (nm)*
1. Cotton (73)	WBM	λ_1	682	682	568	555	615	525	982
except for	(kg/m^2)	$\Delta\lambda_1$	28	28	10	20	175	4	10
yield that	(see Fig. 4)	λ_2	918	845	918	666	925	540	940
has a sample		$\Delta\lambda_2$	20	250	10	5	20	7	10
size of 50	LAI	λ_1	682	550	678	550	568	525	940
	(m^2/m^2)	$\Delta\lambda_1$	15	30	15	50	4	60	10
		λ_2	940	682	865	675	915	540	980
		$\Delta\lambda_2$	60	20	275	50	15	60	10
	yield (lint/ha)	λ_1	540	696	678	540	690	678	670
		$\Delta\lambda_1$	30	4	30	40	10	30	50
		λ_2	678	940	940	684	720	860	970
		$\Delta\lambda_2$	20	20	50	20	20	290	20
2. Potato (25)	WBM	λ_1	550	550	678	682	720	682	615
	(kg/m^2)	$\Delta\lambda_1$	20	30	10	20	30	10	70
		λ_2	682	682	920	940	790	710	935
		$\Delta\lambda_2$	4	26	20	40	20	20	50
	LAI (m^2m^2)	λ_1	682	472	682	678	550	682	625
	(see Fig. 5)	$\Delta\lambda_1$	28	15	28	28	20	7	50
		λ_2	982	790	738	860	688	940	940
		$\Delta\lambda_2$	36	20	45	100	28	30	8
3. Soybean (27)	WBM	λ_1	725	732	696	565	550	635	490
	(kg/m^2)	$\Delta\lambda_1$	25	10	28	50	20	30	75
	(see Fig. 4)	λ_2	845	758	791	875	755	682	682
		$\Delta\lambda_2$	70	10	10	130	10	10	28
	LAI (m^2/m^2)	λ_1	625	495	495	730	682	690	418
		$\Delta\lambda_1$	30	30	30	20	10	40	510
		λ_2	688	685	670	840	790	860	855
		$\Delta\lambda_2$	15	20	40	60	20	100	90
4. Corn (17)	WBM	λ_1	720	505	715	620	620	620	490
	(kg/m^2)	$\Delta\lambda_1$	18	10	4	30	30	30	50
		λ_2	820	645	990	830	1.000	940	825
		$\Delta\lambda_2$	160	6	20	160	30	70	110
	LAI	λ_1	620	550	635	470	495	495	650
	(m^2/m^2)	$\Delta\lambda_1$	20	30	20	8	50	50	4
	(see Fig. 5)	λ_2	590	684	720	740	760	1.000	800
		$\Delta\lambda_2$	10	28	10	2	40	25	165
5. All crops	WBM	λ_1	682	655	525	660	525	640	510
(151)[a]	(kg/m^2)	$\Delta\lambda_1$	30	90	20	30	50	120	100
		λ_2	910	920	682	875	675	880	670
		$\Delta\lambda_2$	20	20	25	250	30	280	60
	LAI (m^2/m^2)	λ_1	540	682	550	682	682	670	490
		$\Delta\lambda_1$	20	10	40	28	35	40	30
		λ_2	682	756	682	910	754	910	965
		$\Delta\lambda_2$	10	20	30	200	40	200	20

Indices are arranged in order of ranking (higher the R^2 value higher is the ranking) and obtained from λ_1 and λ_2 contour plots of R^2 values (see, for example, Figs. 4 and 5). The R^2 values of these models are listed in Table 4.

[a] Includes nine samples from sunflower crop in addition to the cotton (73), potato (25), soybeans (27), and corn (17).

All corn fields were either in late vegetative or critical growth phases (Fig. 1d) resulting in a narrow dynamic rage of their indices. In comparison, cotton, soybeans, and potato had distinctive growth stages (Fig. 1), providing data over a larger dynamic range.

Narrow Band Soil-Adjusted Vegetation Index Relationships with Crop Variables

The narrow band TSAVI indices (Table 2) were computed for the best narrow band NDVI indices of each crop variable to determine if soil adjustment improves R^2 values of the crop models. The TSAVI performed better than the other soil-adjusted indices (see Qi, 1994; Rondeaux et al., 1996; Huete, 1988) and hence is the only soil-adjusted index reported. TSAVI requires site-specific soil line slopes (a) and intercepts (b) (see Lawrence and Ripple, 1998). In this study, a and b are computed using data from 43 soil samples, covering four soil types, by plotting the spectra of two bands (λ_1 and λ_2) involved in best indices and performing best-fit regression. Our re-

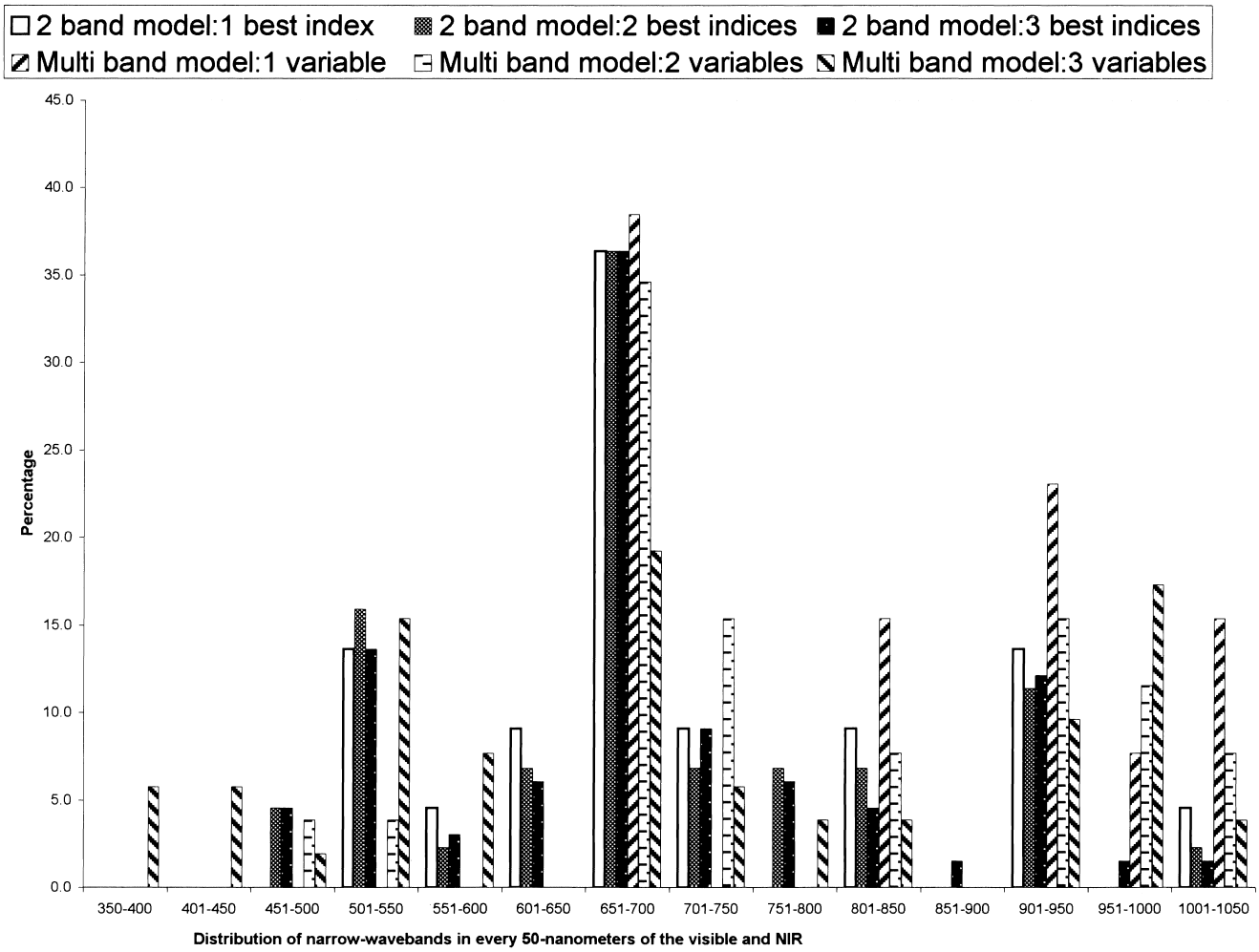

Figure 6. Percentage of occurrences of hyperspectral narrow bands in the three best NDVI models and in three best narrow band four-variable multiple linear models (OMNBR models).

search supports the concept that a well-defined soil line exists for NIR and red. However, there is also a "soil line" for other wavebands such as between green and red (Thenkabail et al. 1999) and other wavebands like red-edge and NIR.

Except in the case of potato WBM, and to a much lesser extent soybean LAI, the increase in R^2 value in soil-adjusted models over the other narrow band NDVI models were insignificant. Potato and soybeans were the two crops with the highest soil background influences. Both of these crops were samples within two very distinct growth stages (see Figs. 1b and c). Of the 25 potato fields, for example, 17 were in early vegetative and eight were in middle or late vegetative (Fig. 1b). The growth stages were identified in the field by experts. The 17 cornfields had about 18% canopy cover. Even the late vegetative fields had only about 35% canopy cover. Below 25% to 35% canopy cover, soil background reflectance is the principal contributor to overall spectral response (Tueller, 1987). Of the 27 soybeans fields, 13 were in early vegetative growth phases with about 40% canopy cover, with the rest having about 90% canopy cover (Fig. 1c). These conditions resulted in potato WBM showing the highest increase in R^2 value (5%) for the narrow band TSAVI models over the best narrow band NDVI models. Generally, soil background effects can be reduced using indices such as TSAVI (Elvidge and Chen, 1995), especially for agricultural crops or homogeneous plant canopies (Rondeaux et al., 1996). However, the soil-adjusted vegetation indices are more significant when agricultural crops are studied on widely varying soils (see, for example, Lawrence and Ripple, 1998). The four soil types in this study area had fine or very fine clayey *Calcixerollic Xerochrept* and *Chromic Calcixerert.* It is likely that the improved sensitivity of these indices become apparent when diverse soil types are studied.

For cotton yield, the soil-adjusted index explained 9% less variability compared to the corresponding narrow band index. This could be attributed to mix of spec-

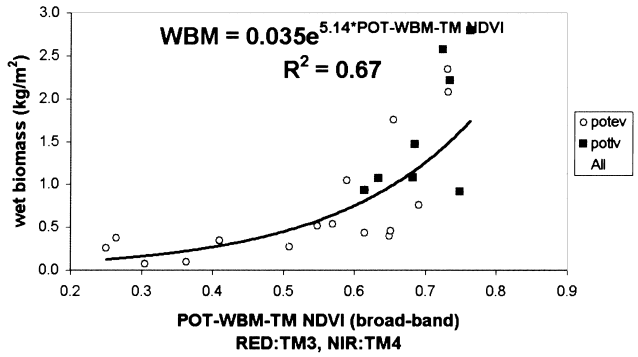

(a) Potato WBM versus best broad-band normalized index

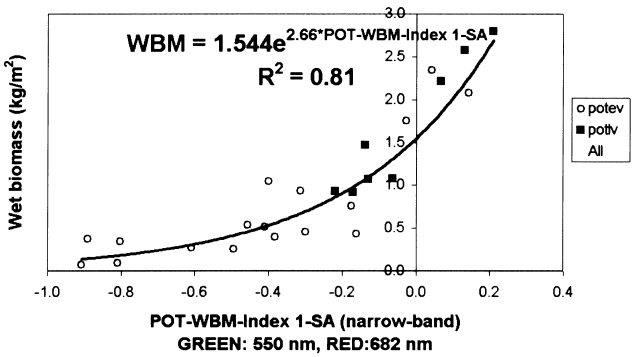

(b) Potato WBM versus best narrow-band normalized index soil adjusted

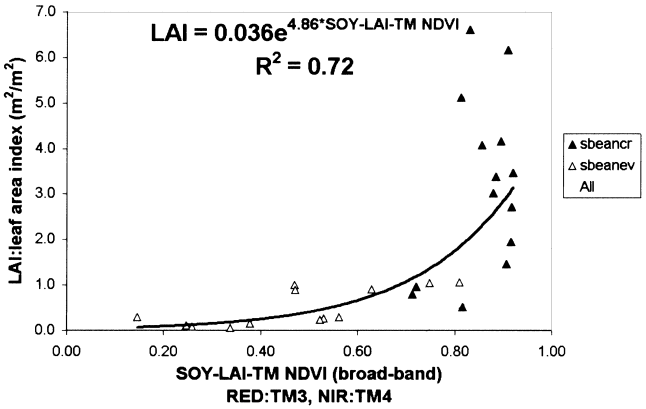

(c) Soybeans LAI versus best broad-band normalized index

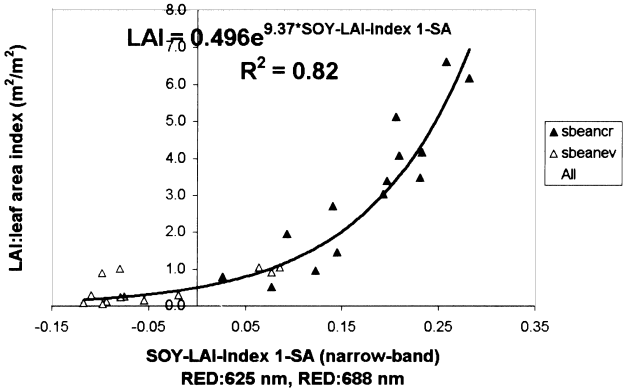

(d) Soybeans LAI versus best narrow-band normalized index soil adjusted

Figure 7. Comparison between the broad band and the narrow band soil-adjusted indices for potato WBM (a and b), and soybeans LAI (c and d). NIR and red-based indices of broad bands (a and c) versus visible band based indices of narrow bands (b and d).

Table 5. R^2 Values of the seven-best NDVIs Reported in Table 3

Crop Parameter Units, (Sample Size)	*Hyperspectral Indices (μm/μm) (Narrow band NDVI Model Ranking)*	*Linear Model R^2 of (Narrow Band NDVI—linear)*	*Nonlinear Exponential Model R^2 of (Narrow Band NDVI—Nonlinear)*	*Percent Increase of the Best Narrow Band NDVI over OMNBR*	*The Best Soil-Adjusted R^2 Narrow Band TSAVI*	*Percent Increase (Positive) or Decrease (Negative) of the Best Narrow Band TSAVI over*	
						The best Broad-band NDVI	*The best Narrow-band NDVI*
1. Cotton WBM	1	0.72	**0.79**	+3	**0.80**	+4	+1
(kg/m^2, 73)	2	0.68	0.72				
	3	0.66	0.71				
	4	0.67	0.67				
	5	0.64	0.67				
	6	0.60	0.57				
	7	0.56	0.56				
	TM-NDVI	0.70	0.76				
2. Cotton LAI	1	0.59	**0.66**	+5	**0.67**	+6	+1
(m^2/m^2, 73)	2	0.59	0.63				
	3	0.53	0.58				
	4	0.53	0.57				
	5	0.48	0.52				
	6	0.44	0.48				
	7	0.41	0.43				
	TM-NDVI	0.53	0.61				
3. Cotton yield	1	**0.64**	0.62	+10	0.55	+1	−9
(Lint/ha, 50)	2	0.61	0.57				
	3	0.59	0.50				
	4	0.54	0.53				
	5	0.54	0.45				
	6	0.50	0.41				
	7	0.46	0.40				
	TM-NDVI	0.54	0.51				
4. Soybeans WBM	1	0.73	**0.84**	+5	**0.84**	+5	0
(kg/m^2, 27)	2	0.71	0.84				
	3	0.68	0.82				
	4	0.68	0.78				
	5	0.68	0.78				
	6	0.68	0.75				
	7	0.65	0.79				
	TM-NDVI	0.59	0.79				

(*continued*)

Table 5. (continued)

Crop Parameter Units, (Sample Size)	*Hyperspectral Indices (μm/μm) (Narrow band NDVI Model Ranking)*	*Linear Model R^2 of (Narrow Band NDVI—linear)*	*Nonlinear Exponential Model R^2 of (Narrow Band NDVI—Nonlinear)*	*Percent Increase of the Best Narrow Band NDVI over OMNBR*	*The Best Soil-Adjusted R^2 Narrow Band TSAVI*	*Percent Increase (Positive) or Decrease (Negative) of the Best Narrow Band TSAVI over*	
						The best Broad-band NDVI	*The best Narrow-band NDVI*
5. Soybeans LAI	1	0.69	**0.80**	+8	**0.82**	+10	+2
(m^2/m^2, 27)	2	0.61	0.77				
	3	0.55	0.76				
	4	0.53	0.68				
	5	0.52	0.75				
	6	0.46	0.73				
	7	0.46	0.73				
	TM-NDVI	0.45	0.72				
6. Potato WBM	1	0.68	**0.76**	+9	**0.81**	+14	+5
(kg/m^2, 25)	2	0.67	0.72				
	3	0.61	0.75				
	4	0.57	0.69				
	5	0.56	0.65				
	6	0.54	0.72				
	7	0.49	0.65				
	TM-NDVI	0.50	0.67				
7. Potato LAI	1	0.67	**0.88**	+10	**0.89**	+11	+1
(m^2/m^2, 25)	2	0.67	0.88				
	3	0.65	0.87				
	4	0.63	0.87				
	5	0.58	0.86				
	6	0.55	0.80				
	7	0.49	0.82				
	TM-NDVI	0.50	0.78				
8. Corn WBM	1	**0.71**	0.59	+12	**0.70**	+11	−1
(kg/m^2, 17)	2	0.69	0.47				
	3	0.65	0.52				
	4	0.59	0.48				
	5	0.59	0.43				
	6	0.54	0.39				
	7	0.47	0.34				
	TM-NDVI	0.59	0.52				

(continued)

Table 5. (*continued*)

Crop Parameter Units, (Sample Size)	*Hyperspectral Indices (μm/μm) (Narrow band NDVI Model Ranking)*	*Linear Model R^2 of (Narrow Band NDVI—linear)*	*Nonlinear Exponential Model R^2 of (Narrow Band NDVI—Nonlinear)*	*Percent Increase of the Best Narrow Band NDVI over OMNBR*	*The Best Soil-Adjusted R^2 Narrow Band TSAVI*	*Percent Increase (Positive) or Decrease (Negative) of the Best Narrow Band TSAVI over*	
						The best Broad-band NDVI	*The best Narrow-band NDVI*
9. Corn LAI	1	**0.86**	0.68	+16	**0.87**	+16	+1
(m^2/m^2, 17)	2	0.80	0.56				
	3	0.77	0.50				
	4	0.71	0.47				
	5	0.68	0.47				
	6	0.68	0.45				
	7	0.63	0.45				
	TM-NDVI	0.70	0.59				
10. All Crops	1	0.43	**0.59**	+5	0.59	+5	0
WBM (kg/m^2, 151,	2	0.41	0.58				
including nine	3	0.39	0.54				
for sunflower)	4	0.39	0.52				
	5	0.38	0.49				
	6	0.35	0.49				
	7	0.35	0.45				
	TM-NDVI	0.40	0.54				
11. All crops	1	0.54	**0.65**	+6	0.65	+6	0
LAI (m^2/m^2, 151,	2	0.48	0.64				
including nine	3	0.40	0.63				
for Sunflower)	4	0.38	0.61				
	5	0.38	0.59				
	6	0.37	0.59				
	7	0.29	0.38				
	TM-NDVI	0.39	0.59				

The R^2 values for the linear and nonlinear hyperspectral narrow band NDVI models and their comparison with: (a) soil-adjusted narrow band TSAVI models and (b) broad band NDVI (TM-NDVI) models.

tral signature from the cotton lint, cotton leaves that are changing color from green to light green or yellowish green, exposed cotton stems (as a result of falling leaves), and some soil background. The narrow band TSAVI models use slopes and intercepts of the soil line to correct for soil background influences only. However, when other factors (e.g., lint, stem, and different shades of leaves) become prominent, the soil adjustment can reduce the accuracy of the prediction.

Other Indices

When a difference index is formulated using two closely spaced band centers, it is indicative of the slope of the reflectance with respect to wavelength and is often referred to as a derivative vegetation index (see Elvidge and Chen, 1995). The "bullseye" areas in Figs 4 and 5, which are on the diagonal, are ideal for computing hyperspectral derivative indices. The first- and second-order derivative spectra (Elvidge and Chen, 1995) were also investigated. The best derivative indices in this study explained 35% to 86% variability in different crop variables, but overall performed significantly poorer than the narrow band and most broad band indices discussed in the previous sections. Hence it is not necessary to report these results in detail. There are indications that the derivative indices are more sensitive to changes in sparsely vegetated and complex (mixture of green and brown) grassland canopies (Elvidge and Chen, 1995; Curran et al., 1990) rather than for crop canopies.

Discrimination of Crop Types and Growth Stages

A knowledge of crop growth stages and crop types (Fig. 1, Table 1) is critical in understanding the reflectivity of different portions of the spectrum. To illustrate this, two TM indices (broad band NDVI and broad band GVI), and three hyperspectral indices (a green and a blue band-based index: narrow band NDVI1; a green and a red band-based index: narrow band NDVI2; and a red and NIR-based index: narrow band NDVI3) were used (Table 1). Statistical tests of significances were performed on mean vegetation indices of the distinctive growth stages (Table 2). The essential notion is that the distribution of sample data may be used to attach confidence levels to spectrally separable classes (Wallace and Campbell, 1989). The mean broad band NDVI for corn (0.67) and cotton (0.66) were about the same (Table 1). Similar insensitivity was detected even when the four TM bands were used in broad band GVI, which provided values of 42.45 for corn and 44.06 for cotton. In comparison, narrow band NDVI1 involving two visible bands provided significant statistical differences (at 95% confidence level) for corn (0.41) and cotton (0.29). Similar, results were obtained using narrow band NDVI2 involving two other visible bands, which had mean values of 0.18 for corn and 0.11 for cotton. Further, the magnitude of differences in one or the other narrow band indices were often higher than broad band NDVI indices. For example, broad band NDVI indices provided significant difference between soybeans (0.67) and potato (0.73) (Table 1). This difference increased when narrow band NDVI2 (0.22 for soybeans and 0.33 for sunflower). Overall, the narrow band NDVI2 provided significant difference between nine combinations of crop types (corn-cotton, corn-potato, corn-sunflower, cotton-potato, cotton-soybean, cotton-sunflower, potato-soybean, potato-sunflower, and soybean-sunflower). In comparison, narrow band NDVI1 provided significant difference for only five combinations, and narrow band NDVI3 with six combinations (Table 1). Compared to this the broad band indices provided significant difference between only three or four combinations of crops. Similar trends can be observed for the growth stages. For example, the broad band NDVI indices were about the same for corn in critical (0.67) and corn in late vegetative (0.67) (Table 1). Compared to this narrow band indices in Table 1 show dramatically improved sensitivities. These results imply that through the use of indices derived from various narrow bands it is possible to maximize crop information. Often information is captured at a specific narrow band better than the other portions depending on phenological and physiographic variability. The results here showed narrow bands centered at 0.550, 0.682, 0.696, 0.920, and 0.468 as most critical for discriminating crops.

Dynamic Range and Saturation of Indices

The "saturation" or upward curvature in plots of WBM or LAI versus a two-band vegetation index is a well-known problem (e.g., Wiegand et al. 1992; Huete et al., 1985). It limits the predictive accuracy of the regression equations. Our own data, as explained in the following paragraphs, shows this behavior strongly. The accepted explanation for saturation is that in dense vegetation, the leaf coverage approaches 100%, while the biomass and LAI continue to grow. Typically, crops reach 100% canopy cover around mid-vegetative phases. However, almost all crops continue to accumulate biomass and LAI until they reach critical phases of growth at which point they begin to senesce. NDVI saturates at LAI of 2.5 to 3 because the amount of red light that can be absorbed by leaves rapidly reaches a peak. In contrast, NIR scattering by leaves continues to increase even as LAI exceeds 3. As a result, once a canopy reaches 100%, NIR reflectance will continue to rise but red reflectance will show only modest decreases, resulting in only slight changes in the ratio (the denominator will have a much greater impact on the ratio than the numerator). For example, consider a canopy that has reached 100%. Red reflectance might be as low as 2%, while NIR could be as high as 50% to 60% depending on the crop (and can-

opy structure). This would lead to an NIR/red ratio of 25 or 30. An increase in LAI might lead to a very slight decrease in red (say to 1.8%) because most of the red reflectance is coming from upper layers of leaves, which have already absorbed all of the light they can. In contrast, NIR reflectance would still increase because leaves are highly transmittant in the NIR and thus additional leaves will still impact NIR scattering. NIR reflectance might still show a substantial increase (say to 55% to 65%) but only generate a modest increase in the ratio (30 to 35), because little change has occurred in the denominator. In order to double the ratio, NIR reflectance would have to nearly double to compensate for little change in red reflectance. Because of this, the indices that have the best chance for overcoming saturation are likely to have red bands, especially in the narrow band portion where red absorption is maximum (an anonymous reviewer contributed to much of this paragraph).

The broad band NIR and red-based indices often have serious problems of saturation. This can be seen in the models of potato WBM (Fig. 7a) and to still greater extent in soybean LAI (Fig. 7c). For potato (Fig. 7a), when WBM is less than 0.7 m^2/m^2 there is a proportional increase in NDVI, showing a clear linear trend. Beyond this value the trend of the plot becomes nonlinear. For soybeans (Fig. 7c), when LAI is less than 1.0 m^2/m^2 there is an proportional increase in NDVI, but beyond this the trend becomes nonlinear, reaching a plateau around LAI of 3.0 m^2/m^2. In such cases, hyperspectral data offers opportunity to scout for band combinations that: (1) offer the best two-band-based NDVI type of relationships (see Figs. 4 and 5) that are often different from the widely used NIR and red-based indices; or (2) perform stepwise linear regressions (Table 3) that help overcome or reduce limitations of saturation in spectral data by incorporating additional information from unique bands from different portions of the spectrum. For example, improved relationships using two visible bands (Figs. 7b and d) compared to commonly used NIR and red-based bands (Figs. 7a and c) are clear. The narrow band centers at 550 nm (green band peak) and 682 nm (red band absorption maxima) in Fig. 7b explained 14% greater variability relative to the broad band NIR and red-based index (Fig. 7a). Similarly, two bands in the red, 625 nm and 688 nm, were found the best in their relationship with soybean LAI (Fig. 7d).

Therefore, in conclusion it can be said that with the broad spectral channels, the most effective measure of leaf cover is an "NDVI type" index using red and NIR. With narrow channels, however, an even better option is available: an index spanning 550 nm to 700 nm where the soil and vegetation have slopes of different signs (see Fig. 1a), resulting in increased sensitivity of indices using this portion of the spectrum (Figs. 7b and d). Other factors like leaf structure, pigmentation, and background effects (litter, weeds), are important, requiring further research in explaining the question of saturation.

Frequently Occurring Optimum Bands

To gain a broad view of the results in this paper, it is useful to consider bands that frequently appear in optimum indices. It can be said that these bands contain an overwhelming fraction of the total crop information in the full spectrum.

The results obtained using narrow band NDVI models (e.g., Tables 4 and 5, Figs. 4 and 5) and OMNBR reflectance models (e.g., Table 3) were used for determining the band centers and widths (see Fig. 6 and Table 6) for estimation of crop biophysical variables. The procedure of obtaining the band centers and band widths was explained previously. The narrow bands that appear in two-band NDVI type models ranked 1, 2, and 3 (see index 1, 2, and 3 in Table 4) and the narrow bands that occur in 1-variable, 2-variable, and 4-variable OMNBR models (Table 3) of different crops were evaluated (Fig. 6). The percentage of these narrow bands in every 50 nm interval were established and their clusters plotted for the 350 nm to 1050 nm (Fig. 6). In both model types, an overwhelming proportion of crop information was in the longer red (650 nm to 700 nm), a particular portion of NIR (900 nm to 950 nm), and a portion of green (500 nm to 550 nm). These were followed by the shorter half of NIR shoulder (800 nm to 850 nm), red-edge (701 nm to 750 nm), and the moisture-sensitive NIR (951 nm to 1000 nm) (Fig. 6). A remarkable 36.4% of all the bands that occur in the first-, second-, and the third-best models of narrow band NDVI type models were clustered in 651 nm to 700 nm region of the spectrum (Fig. 6, Table 4). In the same spectral region, the three best OMNBR models had 19.2% to 38.5% of the entire narrow bands (Fig. 6).

The band widths ($\Delta\lambda_1$, $\Delta\lambda_2$) were determined from the λ_1 versus λ_2 plots such as the ones illustrated in Figs. 4 and 5. The $\Delta\lambda_1$ and $\Delta\lambda_2$ of the three best models (Index 1, Index 2, and Index 3 in Table 4) were used to determine the frequency of occurrence of various band widths as follows:

1. very narrow bands (1 nm to 15 nm), 19 occurrences, 29%
2. narrow bands (16 nm to 30 nm), 32 occurrences, 48%
3. intermediate bands (31 nm to 45 nm), 5 occurrences, 8%
4. broad bands (greater than 45 nm), 10 occurrences, 15%

It is clear from these results that an overwhelming proportion of the bands have narrow (16 nm to 30 nm) or very narrow band (1 nm to 15 nm) widths. For example, the best indices for potato WBM centered at 682 nm and had band width of 4 nm (Table 4). If larger band

Table 6. Recommended Hyperspectral Bands for Agricultural Crop Studies

Band Number	*Wavelength Portion Name*	*Band Center: λ (nm)*	*Band Width: Δλ (nm)*	*Band Description*
1	Blue	495	30	Longer wavelength portion of the blue band. Crop-to-soil reflectance ratio minima for blue and green bands.
2	Green	525	20	Positive change in reflectance per unit change in wavelength of the visible spectrum is maximum around this "green" band (first-order derivative plot of crop spectra will show this).
3		550	20	Green band peak (or the point maximal reflectance) in the visible spectrum. This band can also be centered at 540 nm (providing nearly same results as that of 550 nm). This is the best of the three green bands.
4		568	10	Negative change in reflectance per unit change in wavelength of the visible spectrum is maximum around this "green" wavelength (first-order derivative plot of crop spectra will show this).
5	Red	668	4	Chlorophyll absorption premaxima (or reflectance minima 1). Narrow bands in 668–696 nm portion of the spectrum are most sensitive to crop variables. Of the several narrow bands in this range, specific band centers at 668, 682, and 696 nm are the best.
6		682	4	Greatest crop-soil contrast. Chlorophyll absorption maxima anywhere in 350–1050 nm range of the spectrum (or reflectance minima).
7		696	4	Chlorophyll absorption postmaxima (or reflectance minima 2). This is a point of sudden change in reflectance. Around this point the reflectance begins to change from near-maximal red absorption to beginning of the most dramatic increase in reflectance along the red-edge.
8	Red-edge	720	10	Point on the red-edge around which there is a maximum change in the slope of the reflectance spectra per unit change in wavelength anywhere in the 350–1050 nm (first-order derivative plot of crop spectra will show this).
9	NIR	845	70	Center of "NIR shoulder." A broad band or a narrow band will provide the same result due to near-uniform reflectance throughout the NIR shoulder.
10	NIR peak	920	20	Peak or maximum reflectance region of the NIR spectrum
11	NIR-Moisture sensitive	982	30	Center of the moisture-sensitive "trough" portion of NIR. The "trough" portion (940–1040 nm) had minimum reflectance around 982 nm (or point of maximum "dip" in the trough portion).
12	NIR late	1025	10	Portion of sudden rise in reflectance soon after the moisture-sensitive band.

widths (e.g., $\Delta\lambda_2$=28 nm) are used in models, the R^2 values reduce, often substantially.

The red absorption maximum occurs around 682 nm (optimal band number 6, referred to as λ_6; see Table 6). This is not surprising since the peak absorption for chlorophyll a occurs at this wavelength (Elvidge, 1990; Gates et al., 1965; Grant, 1987). This is the single most frequently occurring narrow band across crops and the variables in both type of models (two-band and multiple linear). The band widths ($\Delta\lambda_1$ or $\Delta\lambda_2$) for the red narrow bands typically range between 4 nm to 28 nm (Table 4). The best suggested band widths for any red narrow band is 4 nm. The other two red narrow bands, λ_5 (668 nm) and λ_7 (696 nm), are of importance depending on crop type, growth stage, and growing conditions, including cultural practices, wherein there is a likelihood of absorption maxima shifting to these bands from the most commonly occurring red absorption maxima band (682 nm). Indeed red absorption varies significantly depending on host of these variables (Elvidge and Chen, 1995; Elvidge, 1990; Carter, 1998; Blackburn, 1998a). Elvidge and Chen (1995) used a 4 nm wide band at 674 nm for red and 780 nm for the NIR to compute the narrow band NDVI for pine canopies. In contrast, Carter (1998) found 701±2 nm for red and 820±2 nm for NIR as the best bands for computing narrow band NDVI for pine canopies but of different varieties. More recently, for grassland canopies Blackburn (1998b) found best correlation with plant pigments when narrow bands (635 nm to 680 nm for red and another narrow band centered at 800 nm for NIR) are used in indices.

One simple hypothesis to explain the dominant role

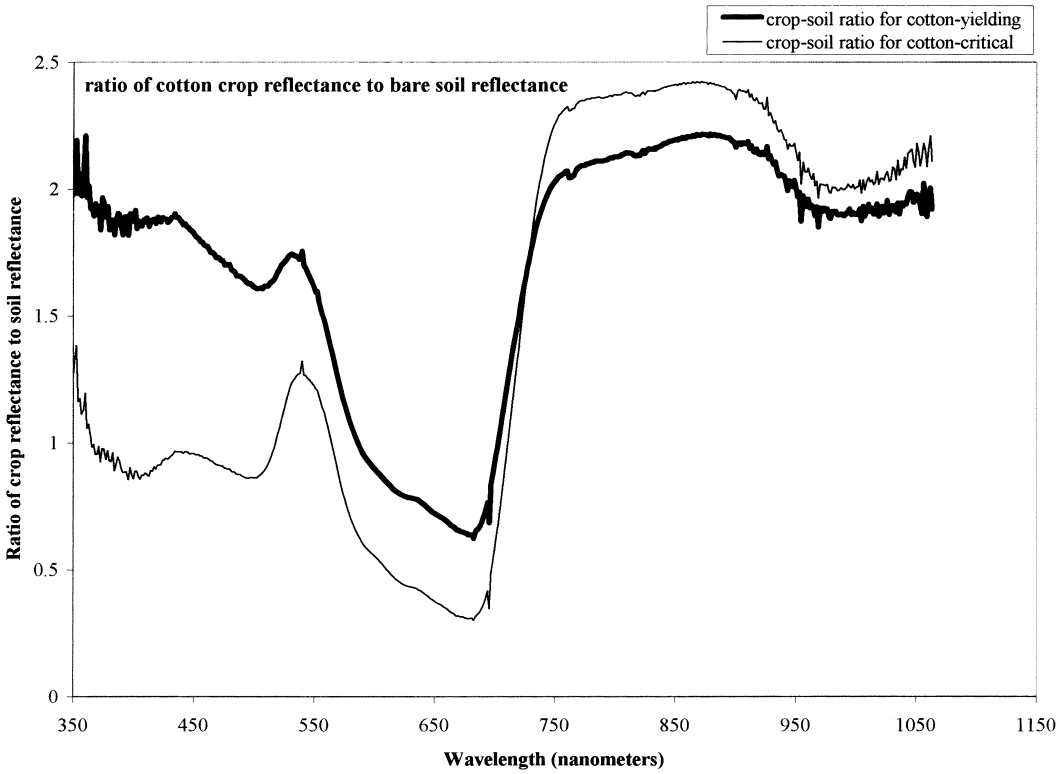

Figure 8. Ratio of cotton crop reflectance to bare soil reflectance.

of the 680 nm band in biophysical correlations is that this band has one of the largest contrasts between leaf and soil reflectance. To illustrate this contrast, we plot the ratio of leaf-to-soil reflectance for cotton as a function of wavelength in Fig. 8. The minimum reflectance ratio is found in a narrow band near 680 nm, for the two advanced growth stages of cotton, while the maximum ratio is a broader band in the longer wavelength portion of NIR. As shown in Fig. 4 and Table 4, it is an index formed from this band combination that gives the best correlation with cotton biomass. Likewise for other crops, indices involving a narrow band (668 nm to 696 nm) occurs frequently, but is not always dominant. Perhaps other biophysical factors such as plant nitrogen content, color, vigor, and structure are important or the smaller sample size for these crops is disturbing the results. The narrow minimum in reflectance ratio at 680 nm is partly due to the decrease in leaf reflectance between 550 nm and 690 nm, but is even more closely associated with the steeply rising soil reflectance in this range (Fig. 1a).

Other narrow bands contributing to optimal indices are listed in Table 6. The λ_{10} (920 nm) is a uniquely centered band that provides peak of NIR reflectance for most crops (e.g., see Fig. 1). The "NIR shoulder" (near-similar reflectance across a range of wavelength) goes from 780 nm to 940 nm for most crops and can be seen for potato (Fig. 1b) and soybeans (Fig. 1c). However, the change in the slope of spectra from 780 nm to 940 nm was highly significant for cotton (Fig. 1a) and to a much lesser extent for corn (Fig. 1d). In most cases the peak NIR reflectance is in the 900 nm to 940 nm region. λ_{11} (982 nm) is "dip" maxima in the 940 nm to 1040 nm portion of the spectrum and is strongly related to change in crop moisture and biomass (see Penuelas et al., 1993). The size of "trough" in 940 nm to 1040 nm region increases with an increase in growth stages (Fig. 1) and is strongly related to biomass.

The λ_3 (550 nm) is the green narrow band at the reflectance peak in the visible range. Narrow bands centered at 540 nm or 550 nm have strong relationships with crop variables (Tables 4 and 5). This region often has maximum crop-to-soil ratio in the visible spectrum (Fig. 8). Since 540 nm and 550 nm are close to one another and have near-similar information, only one of these bands was retained. The band λ_2 (525 nm) is the point of greatest positive change in slope per unit change in wavelength in visible spectrum, and λ_4 (568 nm) is the greatest negative change in slope per unit change in wavelength in visible spectrum for most crops. Similarly, λ_8 (720 nm) represents the point of greatest positive change in slope per unit change in wavelength in red-edge portion of the spectrum. A simple plot of the first-order derivative spectra of each of the crops studied in this paper showed this (the first-order derivative spectral plots are not presented in this paper but can be easily derived from the spectra in Fig. 1). The λ_1=495 nm is the most significant blue band, often with minimal crop-

to-soil reflectance ratio, second only to 680 nm region (Fig. 8). The λ_{12}=1025 nm represents the steep and sudden rise after the moisture sensitive "trough" of the NIR band, which combines with other wave bands to provide optimal information. However, the dark current drift in the spectroradiometer can affect this portion of the spectrum. The NIR shoulder can be represented by a broad band or a narrow band centered at 845 nm (λ_9) to complete the 12 bands. The twelve bands were selected based on their frequency of occurrence in various models of crop variables as discussed throughout this paper. The distribution of the crop information clusters in different waveband portions (Fig. 6) also shows an overwhelming proportion of quantitative crop information in the band centers of these 12 bands (Table 6). Many of the optimum bands that were selected make physical sense given what we know about plant chemistry, canopy structure, and plant spectra (Table 6; Knipling, 1970; Elvidge, 1990). For example, 550 nm is centered over peak chlorophyll reflection in the visible portion of the spectrum, and 982 nm is centered over peak liquid water absorption in the near-infrared.

SUMMARY AND CONCLUSIONS

This research established the optimum number of hyperspectral bands, centers, and widths (Table 6) in the visible and near-infrared spectrum for establishing relationships with agricultural crop biophysical characteristics. This recommendation is based on the study of five crops, nine growth stages, and wide ranging crop characteristics (Table 1). A remarkably strong relationship with crop variables is located in specific narrow bands (Table 6) in the longer wavelength portion of the red, 650 nm to 700 nm, with secondary concentrations in the shorter wavelength portion of the green, 500 nm to 550 nm, in one particular section of the near-infrared, 900 nm to 940 nm, and in the moisture-sensitive near-infrared, centered at 982 nm (Fig. 6). These band regions are followed by red-edge portion centered on 720 nm, and NIR shoulder centered on 845 nm. An overwhelming proportion of these channels had band widths that were classified as: (1) very narrow (1 nm to 15 nm wide) or (2) narrow (16 nm to 30 nm wide). Most were on the order of 10 nm to 20 nm wide (narrow or very narrow). A rigorous procedure adopted here to identify the best narrow band NDVI type models showed that the best two-band combinations often involve (Tables 4 and 6, Figs. 4, and Figure 5): (1) a very narrow red band and a narrow or a broad NIR band, or (2) a very narrow red band and a very narrow or a narrow green band, or (3) a very narrow red band and a narrow band in the moisture-sensitive portion of the NIR, or (4) a very narrow red-edge band and a narrow or broad NIR band. The NIR and red-based NDVI indices are most widely used in remote sensing. This study recommends that the best hyperspectral narrow band NIR and red-based indices can be computed by taking: (1) very narrow band centered at 682 nm ($\Delta\lambda$=4 nm) for red and (2) narrow band centered at 920 nm ($\Delta\lambda$=20 nm) for NIR.

These results demonstrate that the widely used red and NIR band combinations are not necessarily the best for two-band NDVI type indices for estimating crop variables. Even when red and NIR bands are involved, they often appear in unique narrow portions of the spectrum that are not selected by any existing satellite sensor. For example, the index that has highest correlation for cotton WBM had band centers at 682 nm for red and 918 nm for NIR with band widths varying between 20 nm to 28 nm. In comparison Landsat-5 TM bands are centered at 660 nm ($\Delta\lambda$=60 nm) for red (TM3) and at 830 nm ($\Delta\lambda$=140 nm) for NIR (TM4). The dominant role of the waveband centered at 682 nm was partly due to the decrease in leaf reflectance between 550 nm and 690 nm, but is even more closely associated with the steeply rising soil reflectance in this range. The four-variable OMNBR models performed marginally better than the two-band NDVI type models. However, the OMNBR models do not offer the simplicity of the two-band NDVI type models. Also, a significant proportion of the two-band NDVI models perform nearly as well as four-variable OMNBR models. For example, the two-band NDVI models explained between 64% to 88% variability in different crop variables compared to 64% to 92% variability explained by OMNBR models. Most of this variability in OMNBR models is explained using the first two to four narrow bands with addition of further bands adding only small (often, statistically insignificant) incremental increases in R^2 values. Additionally, it was established that when the ratio (M/N) of the number of independent variables or narrow bands (M) to that of total number of field samples (N) exceeds anywhere between 0.15 to 0.20, "over-fitting" of OMNBR models will be a serious problem. The most frequently appearing narrow bands in the four-variable OMNBR models were (Table 3): red (e.g., 682 nm), moisture-sensitive NIR (e.g., 982 nm), green (e.g., 525 nm), and longer portion of NIR (920 nm). The narrow band models perform significantly better than the broad bands. For example, when compared with TM broad band NDVI-type models, the: (1) four-variable OMNBR models explained 3% to 40% additional variability and (2) two narrow band NDVI-type models explained an additional 3% to 16% additional variability. The narrow band transformed soil-adjusted vegetation index (TSAVI) models are considered the best where site specific soil lines are available, but did not provide significant improvements over narrow band NDVI models, except in one case involving potato WBM. The best derivative indices performed significantly poorer than an overwhelming proportion of the narrow band NDVI, OMNBR, and even when compared with most broad band NDVI models.

The study recommends 12 specific narrow bands (Table 6), centers, and widths, which provide optimal crop information in the 350 nm to 1050 nm. These specific bands, centers, and widths are not part of any of the present generation of sensors. The λ_{10} (0.920 μm) is a new uniquely centered band that provides peak of NIR reflectance for most crops, λ_{11} (0.982 μm) is "dip" maxima in the 0.940 to 1.040 μm portion of the spectrum and is in the crop moisture and biomass sensitive portion of the NIR band, λ_6 (0.682 μm) is the peak chlorophyll absorption (least reflectance) portion of the spectrum for most crops and growing conditions with very narrow band width, and λ_3 (0.550 μm) is the green narrow band highlighting the reflectance peak in the visible band portion. The band λ_2 (0.525 μm) is the point of greatest positive change in slope per unit change in wavelength in visible spectrum, and λ_4 (0.568 μm) is the greatest negative change in slope per unit change in wavelength in visible spectrum. Similarly, λ_8 (0.720 μm) represents the point of greatest positive change in slope per unit change in wavelength in red-edge portion of the spectrum. The other two red narrow bands—λ_5 (0.668 μm) and λ_7 (0.696 μm)—are of importance depending on crop type, growth stage, and growing conditions, including cultural practices wherein there is a likelihood of absorption maxima shifting to these bands from the most commonly occurring red absorption maxima band (0.682 μm) as indicated in literature and this study. The λ_1=0.495 μm is the most significant blue band and λ_{12}=1.025 μm represents the steep and sudden rise after the moisture-sensitive "trough" of the NIR band. The NIR shoulder is represented by a broad band centered at 0.845 μm (λ_9) to complete the 12 bands.

The authors would like to thank Prof. Dr Adel El-Beltagy, Director General, and Dr John H. Dodds, Assistant Director General (Research), of the International Center for Agricultural Research in the Dry Areas (ICARDA) for permission and encouragement in carrying out this project. We are grateful for fieldwork support and active participation of Mr. Afif Dakermanji, Dr. Mustafa Pala, Dr. Ahmed Osman, Dr. John Ryan, Mr. A. F. Tarsha, Dr. J. Diekmann, Dr. Mohan Saxena, Dr. Euan Thomson, Mr. Pierre Hayak, Mr. Zuhair Arous, Mr. Haitham Halimeh, Mr. Hisham Salalieh, Mr. Samir Masri, and Mr. Mohammed Salem of ICARDA. Thanks also for the useful discussions provided by our colleagues Dr. Frank Hole, Dr. Nicholos Kouchoukos, Mr. Paul Gluhosky, Mr. Art Gleason (currently in University of Maryland), Mr. Larry Bonneau, Ms. Jane Foster, Mr. Jeff Albert, Dr. Xhui Hui, and Ms. Carrie Howard at the Center for Earth Observation, Yale University. Dr. Steven Skubis provided valuable expertise in producing Figs. 4 and 5. Ms. Tamara Smith provided editorial assistance. Their help is greatly appreciated. Two anonymous reviewers provided many useful comments. We are especially thankful for the reviewer who helped us to provide a better explanation for the sensor saturation. Since the review is anonymous, we are not in a position to quote him/her. The funding for the project comes from the National Aeronautics and Space Administration (NASA) Earth Science Enterprise (formerly, Mission to Planet Earth) grant number NAG5-3853.

REFERENCES

ASPRS. (1995), Land satellite information in the next decade: Data notebook, American Society of Photogrammetry and Remote Sensing (ASPRS), Bethesda, Maryland, USA.

Bartlett, D. S., Hardisky, M. A., Johnson, R. W., Gross, M. F., Klemas, V., and Hartman, J. M. (1988), Continental scale variability in vegetation reflectance and its relationship to canopy morphology. *Int. J. Remote Sens.* 9:1223–1241.

Baset, F., Guyot, G., 2nd Major, d. J. (1989), TSAVI: A vegetation index which minimizes soil brightness effects on LAI and APAR estimation. In *Proceedings of the 12th Canadian Symposium on Remote Sensing*, IGARRS'90, Vancouver, BC, Canada, 10–14 July, 3:1355–1358.

Blackburn, G. A. (1998a), Quantifying chlorophylls and caroteniods at leaf and canopy scales: An evaluation of some hyperspectral approaches. *Remote Sens. Environ.* 66: 273–285.

Blackburn, G. A. (1998b), Spectral indices for estimating photosynthetic pigment concentrations: A test using senescent tree leaves. *Int. J. Remote Sens.*, 19:657–675.

Carter, G. A. (1998), Reflectance bands and indices for remote estimation of photosynthesis and stomatal conductance in pine canopies. *Remote Sens. Environ.* 63:61–72.

Chen, Z., Elvidge, C. D., and Groeneveld, D. P., (1998), Monitoring seasonal dynamics of arid land vegetation using AVIRIS data. *Remote Sens. Environ.* 65:255–266.

Crist, E. P., and Cicone, R. C. (1984), Application of tasselled cap concept to simulated Thematic Mapper data. *Photogramm. Eng. Remote Sens.* 52:81–86.

Curran, P. J., Dungan, J. L., and Gholz, H. L. (1990), Exploring the relationship between reflectance red edge and chlorophyll content in slash pine. *Tree Phys.* 7:33–48.

Elvidge, C. D. (1990), Visible and near infrared reflectance characteristics of dry plant materials. *Int. J. Remote Sens.* 11(10):1775–1795.

Elvidge, C. D., and Chen, Z. (1995), Comparison of broad-band and narrow-band red and near-infrared vegetation indices. *Remote Sens. Environ.* 54:38–48.

Elvidge, C. D., Chen, Z. K., Groeneveld, D. P., 1993. Detection of trace quantities of green vegetation 1990 AVIRIS data. *Remote Sens. Environ.* 44:271–279.

Elvidge, C. D., and Lyon, R. J. P. (1985), Influence of rock-soil spectral variation on the assessment of green biomass. *Remote Sens. Environ.* 17:265–269.

Elvidge, C. D., and Mouat, D. A. (1989), Analysis of green vegetation detection limits in 1989 AVIRIS data. In *Proceedings of the International Symposium of Remote Sensing of Environment, 7th Thematic Conference-Remote Sensing for Exploration Geology*, Calgary, Canada, 10 pp.

Fassnacht, K. S., Gower, S. T., MacKenzie, M. D., Nordheim, E. V., and Lillesand, T. M. (1997), Estimating the leaf area index of north central Wisconsin forests using the Landsat Thematic Mapper. *Remote Sens. Environ.* 61:229–245.

FieldSPEC. (1997), *User's Guide, manual release.* Analytical Spectral Devices, Inc. Boulder, CO.

Friedl, M. A., Michaelsen, J., Davis, F. W., Walker, H., and Schimel, D. S. (1994), Estimating grassland biomass and leaf area index using ground and satellite data. *Int. J. Remote Sens.* 15:1401–1420.

Gates, D. M., Keegan, H. J., Schleter, J. C., Weidner, V. R. (1965), Spectral properties of plants. *App. Opt.* 4:11–20.

Gong, P., Pu, R., Miller, J. R. (1995), Coniferous forest leaf area index estimation along the Oregon transact using compact airborne spectrographic imager data. *Photogramm. Eng. Remote Sens.* 61:1107–1117.

Grant, L. (1987), Diffuse and specular characteristics of leaf reflectance. *Remote Sens. Environ.* 22:309–322.

Huete, A. R. (1988), A soil adjusted vegetation index (SAVI). *Remote Sens. Environ.* 17:37–53.

Huete, A. R., Jackson, R. D., and Post, D. F. (1985), Spectral response of a plant canopy with different soil backgrounds. *Remote Sens. Environ.* 17:37–53.

Idso, B., Pinter, P. J., Jr., R. D. Jackson, and Reginato R. J. (1980), Estimation of grain yields by remote sensing of crop senescence rates. *Remote Sens. Environ.* 9:87–91.

Jackson, R. D. (1983), Spectral indices in n-space. *Remote Sens. Environ.* 13:409–421.

Kauth, R. J., and Thomas, G. S. (1976), The tasselled cap-a graphic description of the spectral-temporal development of agricultural crops as seen by Landsat. In *Proceedings, Symposium on Machine Processing of Remotely Sensed Data*, pp. 41–51.

Knipling, E. B. (1970), Physical and physiological basis of the reflectance of visible and near-infrared radiation. *Remote Sens. Environ.* 1:155–159.

Lawrence, R. L., Ripple W. J. (1998), Comparisons among vegetation indices and bandwise regression in a highly disturbed, heterogeneous landscape: Mount St. Helens, Washington. *Remote Sens. Environ.* 64:91–102.

Lyon, J. G., Yuan, D., Lunetta, R. S., and Elvidge, C. D. (1998), A change detection experiment using vegetation indices. *Photogramm. Eng. Remote Sens.* 62:143–150.

Moran, S. M., Clarke, T. R., Inoue, Y., and Vidal, A. (1994), Estimating crop water deficit using the relationship between surface-air temperature and spectral vegetation index. *Remote Sens. Environ.* 49:246–263.

Penuelas, J., Filella, I., Biel, C., Serrano, L., and Save, R. (1993), The reflectance at the 950–970 region as an indicator of plant water status. *Int. J. Remote Sens.* 14:1887–1905.

Qi, J., Chehbouni, A., Huete, A. R., Kerr, Y. H., and Sorooshian, S. (1994), A modified soil adjusted vegetation index (MSAVI). *Remote Sens. Environ.* 48:119–126.

Ripple, W. J. (1994), Determining coniferous forest cover and forest fragmentation with NOAA-9 advanced very high resolution radiometer data. *Photogramm. Eng. Remote Sens.* 60:553–540.

Rondeaux, G., Steven, M., and Baret, F. (1996), Optimisation of soil-adjusted vegetation indices. *Remote Sens. Environ.* 55:95–107.

Rouse, J. W., Jr., Haas, R. H., Schell, J. A., 2nd Deering, D. W. (1973), Monitoring vegetation systems in the great plains with ERTS. In *Third ERTS symposium, NASA SP-351, U.S. Govt. Printing Office*, Washington, D.C., vol. 1, pp. 309–317.

Running, S. W. (1989), Estimating terrestrial primary productivity by combining remote sensing and ecosystem simulation. In *Remote Sensing of Biosphere Functioning, Ecological Studies 79* (R. J. Hobbs and H. A. Mooney, Eds.), Springer-Verlag, New York, pp. 65–86.

Ryan, J., Masri, S., Garabet, J., Diekmann, J., and Habib, H. (1997), *Soils of ICARDA's agricultural experimental stations and sites: Climate, classification, physical and chemical properties, and land use*, International Center for Agricultural Research in the Dry Areas (ICARDA), Aleppo, Syria.

SAS Institute. (1997a), *SAS/IML User's Guide and Software Release 6.12.* SAS Institute Inc, Cary, NC.

SAS Institute. (1997b), *SAS/STAT User's Guide and Software Release 6.12.* SAS Institute Inc, Cary, NC.

Shibayama, M., and Akiyama T. (1991), Estimating grain yield of maturing rice canopies using high spectral resolution reflectance measurements. *Remote Sens. Environ.* 36:45–53.

Shibayama, M., Takahashi, W., Morinaga, S., and Akiyama, T. (1993), Canopy water deficit detection in paddy rice using high resolution field spectroradiometer. *Remote Sens. Environ.* 45:117–126.

Stoney, W. E., and Hughes, J. R. (1998), A new space race is on! *GIS World* 11:44–46.

Thenkabail, P. S., Smith, R. B., and De Pauw, E. (1999), Hyperspectral vegetation indices for determining agricultural crop characteristics. CEO research publication series No. 1. Center for Earth Observation, Yale University Press, New Haven, CT.

Thenkabail, P. S., Ward, A. D., and Lyon, J. G. (1995), Landsat-5 Thematic Mapper models of soybean and corn crop characteristics. *Int. J. Remote Sens.* 15:49–61.

Tucker, C. J. (1977), Spectral estimation of grass canopy variables. *Remote Sens. Environ.* 6:11–26.

Tucker, C. J. (1979), Red and photographic infrared linear combinations for monitoring vegetation. *Remote Sens. Environ.* 8:127–150.

Tueller, P. T. (1987), Remote sensing science application in arid environments. *Remote Sens. Environ.* 23:143–154.

Wallace, J. F., and Campbell, N. (1989), Analysis of remotely sensed data. In *Remote Sensing of Biosphere Functioning, Ecological Studies 79* (R. J. Hobbs, H. A. Mooney, Eds.), Springer-Verlag, New York, pp. 291–304.

Wheeler, S. G., and Misra, P. N. (1976), Linear dimensionality of Landsat agricultural data with implications for classifications. In *Proceedings, Symposium on Machine Processing of Remotely Sensed Data*, West Lafayette, IN, Laboratory for the Applications of Remote Sensing.

Wiegand, C. L., Mass, S. J., Aase, J. K., Hatfield, J. L., Pinter, P. J., Jr., Jackson, R. D., Kanemasu, E. T., Lapitan, R. L. (1992), Multisite analysis of spectral-biophysical data for wheat. *Remote Sens. Environ.* 42:1–21.

Wiegand, C. L., and Richardson A. J. (1990), Use of spectral vegetation indices to infer leaf area, evapotranspiration, and yield: I. Rationale. *Agron. J.* 86:623–629.

Wiegand, C. J., Richardson, A. J., Escobar, D. E., and Gerbermann, A. H. (1991), Vegetation indices in crop assessments. *Remote Sens. Environ.* 35:105–119.